



**HAL**  
open science

## Homeostatic and Tissue Repair Defaults in Mice Carrying Selective Genetic Invalidation of CXCL12/Proteoglycan Interactions.

Patricia Rueda, Adèle Richart, Alice Récalde, Pamela Gasse, José Vilar, Coralie Guérin, Hugues Lortat-Jacob, Paulo Vieira, Françoise Baleux, Fabrice Chretien, et al.

► **To cite this version:**

Patricia Rueda, Adèle Richart, Alice Récalde, Pamela Gasse, José Vilar, et al.. Homeostatic and Tissue Repair Defaults in Mice Carrying Selective Genetic Invalidation of CXCL12/Proteoglycan Interactions.. *Circulation*, 2012, 126 (15), pp.1882-95. 10.1161/CIRCULATIONAHA.112.113290 . pasteur-00743099

**HAL Id: pasteur-00743099**

**<https://pasteur.hal.science/pasteur-00743099>**

Submitted on 15 Apr 2013

**HAL** is a multi-disciplinary open access archive for the deposit and dissemination of scientific research documents, whether they are published or not. The documents may come from teaching and research institutions in France or abroad, or from public or private research centers.

L'archive ouverte pluridisciplinaire **HAL**, est destinée au dépôt et à la diffusion de documents scientifiques de niveau recherche, publiés ou non, émanant des établissements d'enseignement et de recherche français ou étrangers, des laboratoires publics ou privés.

**HOMEOSTATIC AND TISSUE REPARATION DEFAULTS IN MICE CARRYING,  
SELECTIVE, GENETIC INVALIDATION OF CXCL12/PROTEOGLYCAN  
INTERACTIONS**

**Rueda et al:** CXCL12/proteoglycan interactions in angiogenesis

Patricia Rueda, PhD <sup>1\*</sup>, Adèle Richart MsC <sup>2,3\*</sup>, Alice Récalde PhD <sup>2,3\*</sup>, Pamela Gasse PhD <sup>1</sup>,  
José Vilar PhD <sup>2,3</sup>, Coralie Guérin MsC <sup>2,3</sup>, Hugues Lortat-Jacob PhD <sup>4</sup>, Paulo Vieira PhD <sup>5</sup>,  
Françoise Baleux PhD <sup>6</sup>, Fabrice Chretien MD, PhD <sup>7</sup>, Fernando Arenzana-Seisdedos MD <sup>1‡</sup>,  
Jean-Sébastien Silvestre PhD <sup>2,3‡</sup>

<sup>1</sup>Institut Pasteur, Unité de Pathogénie Virale, Département de Virologie, INSERM U819,  
Paris, France

<sup>2</sup>INSERM UMRS 970, Paris Cardiovascular Research Center, Paris, France

<sup>3</sup>Université Paris Descartes, Sorbonne Paris cité, Paris, France

<sup>4</sup>CEA, CNRS, Université Joseph Fourier – Grenoble 1, Institut de Biologie Structurale Jean-  
Pierre Ebel, UMR 5075, 38000 Grenoble, France

<sup>5</sup>Institut Pasteur, Unité de Lymphopoïèse. INSERM U688, Paris, France

<sup>6</sup>Institut Pasteur, Unité de Chimie des Biomolécules. Centre National de la Recherche  
Scientifique 2128, Paris, France

<sup>7</sup>Institut Pasteur, Unité Histopathologie Humaine et Modèles Animaux, Département  
Infection et Epidémiologie, Paris, France; Université Versailles Saint Quentin en Yvelines,  
Faculté de Médecine ; Assistance Publique – Hôpitaux de Paris, Hôpital Raymond Poincaré,  
Paris, France

\*Authors have equally contributed to this work

≠Authors have equally contributed to this work

‡Correspondence should be addressed to Fernando Arenzana-Seisdedos: INSERM U819;  
Unité de Pathogénie Virale; Département de Virologie ; Institut Pasteur ; 28, Rue du Dr. Roux  
; 75724 Paris Cedex

Total word count: 6994

Subject code: 129

## ABSTRACT

**Background.** Interaction with heparan sulfate (HS) proteoglycans is supposed to provide chemokines with the capacity to immobilize on cell surface and extracellular matrix for accomplishing both tissue homing and signalling of attracted cells. However, the consequences of the exclusive invalidation of such interaction on the roles played by endogenous chemokines *in vivo*, remains unascertained.

**Methods and results.** We engineered a mouse carrying a *Cxcl12* gene (*Cxcl12<sup>Gagtm</sup>*) mutations that preclude interactions with HS structures while they do not affect CXCR4-dependent cell-signalling of CXCL12 isoforms ( $\alpha, \beta, \gamma$ ). *Cxcl12<sup>Gagtm/Gagtm</sup>* mice develop normally, express normal levels of total and isoform-specific *Cxcl12* mRNA and show increased counting of circulating CD34+ haematopoietic precursor cells. Following induced acute ischemia, a marked impaired capacity to support revascularization was observed in *Cxcl12<sup>Gagtm/Gagtm</sup>* animals associated to a reduced number of infiltrating cells in the ischemic tissue despite the massive expression of CXCL12 isoforms. Importantly, exogenous administration of CXCL12 $\gamma$ , which binds HS with the highest affinity ever reported for a cytokine, fully restores vascular growth, while HS-binding CXCL12 $\gamma$  mutants failed to promote revascularization in *Cxcl12<sup>Gagtm/Gagtm</sup>* animals.

**Conclusions.** These findings prove the role played by HS-interactions in the functions of CXCL12 both in homeostasis and physiopathological settings and document originally the paradigm of chemokine-immobilisation *in vivo*.

**Keywords :** Angiogenesis, Ischemia, Chemokines, Proteoglycans, CXCL12

## INTRODUCTION

Chemokines control the migration of a large array of cells, thus regulating function and homeostasis of a number of tissues. Glycosaminoglycans (GAG), the glycanic moiety of proteoglycans, are considered as the critical biological structure that determines the immobilisation of chemokines on the extracellular matrix and cell surfaces. Immobilisation provides chemokines with a robust anchoring against blood flow and, by restraining their diffusion, facilitates both the formation of local gradients and the synchronous coordination of motility and cell adhesion<sup>1 2 3</sup>.

Among GAG, chemokines bind preferentially to heparan sulfate (HS) through interactions either of canonical BBXB and BBBXB (B, basic; X, any residue) or discontinuous cationic protein epitopes, with the negatively charged sulfated residues of HS<sup>4</sup>. Although chemokine binding to GAGs has been well described from a biochemical point of view, the functional aspects of these interactions remain poorly understood and *in vivo* investigations to address the importance of chemokine-GAG interactions are limited. In some cases the experimental approach, like the administration of sulfated glycans competing exclusively with HS<sup>5</sup> or the genetic interference selectively inhibiting endothelial HS biosynthesis<sup>6</sup>, have broad effects and would affect, beyond chemokines, the interaction of GAG with many other factors. In other cases, the overlapping or spatial proximity of chemokine domains involved in receptor-mediated cell signalling and GAG-attachment has obscured interpretation and significance of the results obtained by exogenous administration of GAG-binding mutant chemokines with reduced agonist capacity<sup>7</sup>.

In this regard, CXCL12 is unique among chemokines for the spatial separation between the receptor- and HS-binding sites, localized on the opposite sides of the molecule<sup>8</sup>, thus permitting the evaluation of the contribution of each domain to their biological functions.

In mice three isoforms (CXCL12 $\alpha$ , CXCL12 $\beta$  and CXCL12 $\gamma$ ), that show an exceptional degree of interspecies conservation exceeding 95% homology for their amino-acid sequences, are generated by alternative splicing<sup>9 10</sup>. CXCL12 $\beta$  and CXCL12 $\gamma$  contain the entire amino-acid sequence (68Aa) of CXCL12 $\alpha$  which encompasses the CXCR4-binding domain and the protein core BBXB motif (K24H25L26K27) critically required for the HS-binding. CXCL12 $\beta$  (72Aa) and CXCL12 $\gamma$  (98Aa) differs from CXCL12 $\alpha$  by the addition of the last four and thirty Aa, respectively encoding one and four additional BBXB motifs. While CXCL12 $\alpha$  and CXCL12 $\beta$  display affinities for HS or heparin in the same range of magnitude ( $K_D$ , 93 and 25nM, respectively), that of CXCL12 $\gamma$  is 1.5 nM and constitutes the strongest HS-affinity ever measured for a cytokine<sup>11 12</sup>. This firm interaction with HS relies on the cooperativeness of the core and the high cationic C-ter domain of the chemokine, where the four overlapping BBXB motifs of CXCL12 $\gamma$  mostly accounts for the slow off-rates from immobilized HS<sup>12</sup>.

We reported previously that neutralisation of the K24H25L26K27 cationic charge (K24S and K27S substitutions) is sufficient to drastically reduce binding to HS and complexing of CXCL12 $\alpha$  either with immobilized-heparin or HS<sup>11 12 13 14</sup>. Similarly, O'Boyle *et al* recently reported that combined K24S and K27S in CXCL12 $\beta$ , are sufficient to impede HS-binding of this isoform on the apical surface of endothelial cells and promote a dramatic blood and delayed clearance as compared to the WT counterpart<sup>15</sup>. To abrogate HS-binding of CXCL12 $\gamma$ , the combined mutation of K24H25L26K27 and the C-ter four overlapping BBXB motifs is therefore required<sup>12 13</sup>. Of note, while all these HS-binding CXCL12 mutants show a preserved global structure defined by Nuclear Magnetic Resonance<sup>11 12</sup> and are full CXCR4 agonists *in vitro*<sup>11 10 12 13 15</sup>, they have only a marginal capacity to attract leukocytes or endothelial progenitor cells *in vivo* and are unable to immobilise and localise properly on

GAG structures<sup>13 15</sup>. Importantly, CXCL12 HS-binding mutants induce homologous CXCR4 desensitisation thus neutralising the chemoattractant properties of CXCL12 WT molecules<sup>15</sup>. CXCL12 binds both CXCR4 and CXCR7<sup>16 17 18 19</sup>, is the only cognate ligand of CXCR4, and plays essential and non-redundant roles in organogenesis<sup>20 21</sup>. CXCL12 is widely expressed by mesothelial, epithelial, endothelial and osteoblasts as well as bone marrow (BM) stromal cells<sup>22 23 24</sup>. It acts in post-natal life as a key chemoattractant for haematopoietic progenitor cells (HPC) and leukocytes<sup>24 16 17</sup> and regulates the BM homing and retention/egress of haematopoietic cells<sup>25 26</sup> as well as the basal trafficking and transendothelial migration of leukocytes<sup>27 28 29</sup>. Aside from homeostasis, CXCL12 is involved both in tumorigenesis and cancer metastasis<sup>30</sup> and is a pathogenic factor in systemic disease like rheumatoid arthritis where it shows proangiogenic and inflammatory effects<sup>31</sup>. In addition, CXCL12 plays a role of paramount importance as an essential and non-redundant factor involved in tissue remodelling, in particular in vascular regeneration<sup>32</sup>.

Overall, the structural characteristics and pleiotropic roles played by CXCL12 make it ideally suited for investigating how the interactions with GAG/HS modulate the biological role of a chemokine *in vivo*. To this aim, we engineered a transgenic mouse expressing a *Cxcl12* gene where the critical sequences encoding CXCL12 domains involved in HS-binding are selectively invalidated while preserving intact the CXCR4-agonist potency and efficiency of the mutant proteins. The mutant mice show enhanced serum levels of free CXCL12 and an increased number of circulating leukocytes and CD34+ haematopoietic cells<sup>5</sup>. Strikingly, and in keeping with the essential role played by CXCL12 in tissue repair, these mice display a dramatically reduced capacity to regenerate vascular growth following acute ischemia that is recovered by expression of WT CXCL12 demonstrating the importance of GAG binding for proper *in vivo* function. This is the first description to our knowledge of an animal model where the HS-binding capacities of an endogenous chemokine were genetically invalidated

and the consequences of the selectively impaired function investigated both in homeostasis and physiopathological settings.

## METHODS

Experiments were conducted according to the French veterinary guidelines and those formulated by the European Community for experimental animal use (L358-86/609EEC).

**Chemokines: cDNA expression vectors and synthesis.** Tissues were obtained by dissection of *Cxcl12*<sup>Gagtm/Gagtm</sup> mice or WT littermates previously sacrificed by cervical dislocation. Bone marrow was recovered from right tibiae by the flushing procedure using 5ml PBS. Total RNAs were purified using the RNeasy Kit (Qiagen), and *Cxcl12* cDNAs were synthesized using 0.5µg of the corresponding RNAs with random hexamer. The isoform-specific *Cxcl12* cDNA corresponding to WT and *Cxcl12*<sup>Gagtm/Gagtm</sup> mice were generated as described previously<sup>13</sup> using the *Cxcl12* primers: forward common, 5'-cacccatggagccaaggtcgtcgcc-3' and the reverse, 5'-ttacttgttaaagctttctccaggta-3', 5'-tcacatcttgagcctctgtttaaagc-3' and 5'-ctagttttcttttctgggcagcc-3' for *Cxcl12*α, *Cxcl12*β and *Cxcl12*γ.

The coding CXCL12γm2 DNA was derived by mutagenesis from the WT sequence. All of them were subcloned in a CMV-promoter driven pcDNA3 expression vector (InVitrogen). HEK293 cells were transfected with CXCL12-expression vectors to generate CXCL12-containing cell supernatants. Chemically synthesized chemokines were generated and evaluated for their purity and concentration as previously described<sup>11</sup>.

***Cxcl12* knock-in and *Cxcl12*<sup>Gagtm</sup> mouse generation.** A 14.5 kb genomic DNA used to construct the targeting vector was first subcloned from a positively identified C57BL/6 BAC clone (Dr. A. Lu. iTI, Fresh Meadows, New York, USA). The AAG > TCG and AAA > TCT (aa: K > S) mutations within exon 2, as well as the stop codon TAG insertion in exon 4, that selectively prevents translation of CXCL12γ last 30Aa, were generated by 3-step PCR mutagenesis. The PCR fragments carrying mutations were then used to replace the WT

sequence using conventional subcloning methods. The long homology arm extends ~6.6 kb 5' to the first set mutations in exon 2. The LoxP/FRT-Neo cassette was inserted ~2.2 kb downstream of the first set mutations, and ~2.3 kb upstream of the second set mutations (stop codon insertion in exon 4) in intron 3-4. The short homology arm extends 3.3 kb 3' to the second set mutations. The targeting vector (backbone, a 2.4 kb pSP72 based vector) was validated by restriction analysis and sequencing after each modification. Ten micrograms of the targeting vector was linearized by Cla I digestion and then transfected by electroporation of BA1 (C57BL/6 x 129/SvEv) hybrid embryonic stem cells. After selection with G418 antibiotic, surviving clones were expanded for PCR analysis to identify recombinant ES clones and a secondary confirmation of positive clones identified by PCR was performed by Southern Blotting analysis. Targeted BA1 (C57BL/6 x 129/SvEv) hybrid embryonic stem cells were microinjected into C57BL/6 blastocysts. Resulting chimeras with a high percentage agouti coat colour were mated to wild-type C57BL/6 mice to generate F1 *Cxcl12*<sup>Gagtm/wt</sup> offspring. Tail DNA was analyzed by PCR to confirm the integration of the desired sequences. The obtained *Cxcl12*<sup>Gagtm/wt</sup> animals, mice were crossed with transgenic 129sv PGK-Cre for LoxP/FRT-Neo cassette excision. Offspring that do not inherit PGK-CRE and delete LoxP/FRT-Neo cassette were selected and the colony was amplified. Identification of genotypes of mice encoding *Cxcl12*<sup>Gagtm</sup> upon excision of Neo-cassette was performed by PCR with forward, 5'tgccagcataaagacactccg3' and reverse 5'cagcccttgaagtaatcactgc 3' primers.

**Characterisation of *Cxcl12* mRNA and protein expression in normal and ischemic tissues.** For quantitative real time PC, cerebellum, brain, thymus, heart and skeletal muscle tissues were obtained by dissection of *Cxcl12*<sup>Gagtm/Gagtm</sup> mice or WT littermates. Bone marrow was recovered from right tibiae by the flushing procedure using 5ml PBS. Total RNAs were purified using the Rneasy Kit (Qiagen) according to the manufacturer instructions, and

cDNAs were synthesized using 0.5µg of the corresponding RNAs with random hexamer. Quantitative real time-PCR was performed in a Mix3005Tm QPCR System with a MxPro QPCR Software 3.00 (Stratagene, La Jolla, CA) and SYBR Green detection system, using the forward common primer 5'tgccttcagattgttgac3' and the reverse primers 5'ccacggatgtcagccttcc3', 5'cttgagcctctgtttaagctt3', or 5'gctagcttacaagcgccagagcagagcgcactgcg3' for *Cxcl12α*, *Cxcl12β* or *Cxcl12γ*, respectively. Mouse HPRT and GAPDH genes were used as controls. Quantitative analysis was then performed using the Livak method.

For evaluating CXCL12 accumulation and localisation in muscle, frozen sections (7 µm) were incubated with CXCL12 mAb K15C (10µg/ml) antibodies, FITC-Griffonia Simplicifolia Agglutinin isolectin B4 (1:100, Sigma) and rabbit anti-mouse alpha smooth muscle actin (1:100, Abcam) at room temperature. Finally, sections were incubated with DAPI (1:10,000, Sigma). Alexa fluor 594 (Invitrogen, 1:100) and Cy5-labeled secondary antibodies (1:200, Jackson ImmunoResearch) were then used to reveal CXCL12 and alpha actin-positive stainings, respectively

Quantification of CXCL12 in mice blood serum was carried out using the DuoSet ELISA Development kit for mouse CXCL12 (R&D Systems, MN, USA). Blood was collected by cardiac puncture.

**Cell surface binding potential and chemotaxis assay.** Evaluation of synthetic CXCL12 chemokines adsorption on cell surfaces of CHO GAG-expressing cells and chemotaxis assay (human CD4<sup>+</sup> T lymphocytes or human endothelial progenitor cells (EPC), were performed as described previously<sup>11 13</sup>. EPC were isolated from human umbilical cord blood and differentiated *ex vivo*, as previously described<sup>33</sup>.

**Peripheral blood analysis.** WT and *Cxcl12*<sup>Gagtm/Gagtm</sup> mice (n=10) were killed and blood collected as described above and transferred to EDTA pre-treated tubes (Sarstedt). Then, 20µl of sample were collected using the disposable diluting pipette system of the BD Unopette procedure (BD, NJ, USA). Cells were stained using the Gr1-FITC, CD4-PB and CD34-PE antibodies or the matching control isotypes and analyzed in a BD FACS Canto Flow Cytometer (BD Bioscience). Erythrocytes and Thrombocytes were quantified by flow cytometry (Siemens ADVIA 120).

### **Experimental model of surgically-induced hindlimb ischemia.**

**Induction of ischemia and plasmids electrotransfert.** *Cxcl12*<sup>Gagtm/Gagtm</sup> mice and their wild-type C57BL/6 littermate underwent surgical ligation of the proximal part of the right femoral artery, above the origin of the circumflexa femoris lateralis. 50µg of expression plasmids encoding for CXCL12 $\alpha$ , CXCL12 $\gamma$  or CXCL12 $\gamma$ m2 were then injected into both tibial anterior and gastrocnemius muscles of the anesthetized mouse, as previously described<sup>34</sup>. Transcutaneous electric pulses (8 square-wave electric pulses of 200 V/cm, 20 ms each, at 2 Hz) were delivered by a PS-15 electropulsator (Jouan) using two stainless steel plate electrodes placed 4.2 to 5.3 mm apart, at each side of the leg. The left leg was not ligated neither electrotransferred and was used as an internal control. In additional set of experiments, C57BL/6 mice with surgically-induced hindlimb ischemia and treated with expression plasmids also received intravenous injection of  $1.10^5$  human EPC.

**Analysis of neovascularization.** Post-ischemic neovascularisation was evaluated by three different methods, as previously described<sup>34</sup>.

*Microangiography.* Mice were anesthetized (pentobarbital) and longitudinal laparotomy was performed to introduce a polyethylene catheter into the abdominal aorta and inject contrast medium (Barium sulphate, 1 g/mL). Angiography of hindlimbs was then performed and

images (two per animals) were acquired using a high-definition digital X-ray transducer. Images were assembled to obtain a complete view of the hindlimbs.

*Capillary and arteriole density analysis.* Frozen tissue sections (7  $\mu\text{m}$ ) from calf muscle were incubated with rabbit polyclonal antibody directed against total fibronectin (dilution 1:50, Abcys) to identify capillaries and rabbit anti-mouse alpha smooth muscle actin (dilution 1/100, abcam) to identify arterioles. The capillary-to-myocytes ratio was determined in both ischemic and non ischemic legs.

*Laser Doppler Perfusion Imaging.* Briefly, excess hairs were removed by depilatory cream from the limb, and mice were placed on a heating plate at 37°C to minimize temperature variation. Nevertheless, to account for variables, including ambient light, temperature, and experimental procedures, perfusion was calculated in the foot and expressed as a ratio of ischemic to non ischemic legs.

#### **Analysis of cell infiltration in the ischemic tissue.**

To evaluate the number of infiltrating CD45.1-positive cells,  $10^7$  mononuclear cells isolated from the bone marrow of CD45.1 mice were intravenously injected to *Cxcl12<sup>Gagtm/Gagtm</sup>* mice and their wild-type C57BL/6 littermate, 1 day after femoral artery ligation. Five days after the injection, the ischemic gastrocnemius muscles were harvested, weighed, minced and digested in 450 U/ml Collagenase I, 125 U/ml Collagenase XI, 60 U/ml DNase I and 60 U/ml hyaluronidase (Sigma Aldrich) for 1 hour at 37°C. After Ficoll separation, infiltrating cells were stained with CD45.1-PerCPCy5.5, CD34-APC and CXCR4-PE and analyzed using a FACS Aria (BD).

To measure the number of infiltrating EPC, the ischemic gastrocnemius muscles were digested as described above. The number of cells being positive for  $\beta$ 2-microglobuline anti-human FITC (Biolegend, 1:200) and DAPI was then evaluated on a LSRII Flow Cytometer

(Becton Dickinson). In a third set of experiment, 10-week wild-type C57BL/6 mice underwent medullar aplasia by total body irradiation (9.5 gray). Bone marrow cells were then isolated from femurs and tibias of GFP C57BL/6 mice and intravenously injected in irradiated animals. After 8 weeks, mice underwent surgical ligation of the proximal part of the right femoral artery, as described above. The gastrocnemius muscles were then harvested 2 days after ischemia. Infiltrating circulating BM-derived GFP-positive cells were detected by fluorescent microscopy and their endothelial cell phenotype revealed by costaining with rhodamine Griffonia Simplicifolia Agglutinin isolectin B4 (1:100, Sigma) and their inflammatory phenotype by co-staining with rat anti-mouse Mac-3 (BD pharmingen, 1:300) and donkey anti-rat RITC (Jackson ImmunoResearch, 1:200).

**Statistical Analysis.** Statistical analysis were performed using StatView. Kruskal Wallis analysis of variance was used to compare each parameter. Bonferroni-corrected Mann-Whitney tests were then performed to identify which group differences account for the significant overall Kruskal Wallis. Results were expressed as mean  $\pm$  SEM. A value of  $p < 0.05$  was considered significant.

## RESULTS

We have engineered mice encoding a *Cxcl12* gene carrying mutations (Figure 1A and S1) that drastically reduce CXCL12/HS interactions as deduced from biochemical and biophysical measurements and functional assays *in vitro* and *in vivo*<sup>11 12 13 15</sup>. K24S and K25S point mutations were introduced in the critical HS-binding domain (encoded in the second exon) shared by the three CXCL12 isoforms (Figure S2(A)). Furthermore, a nonsense *amber* mutation was introduced in the fourth exon to prevent the translation of the distinctive, thirty-last Aa of the highly cationic C-ter domain of CXCL12 $\gamma$  (Figure S1(A)). We opted for this strategy to avoid unpredictable consequences in the expression of a heavily CXCL12 $\gamma$  mutated protein carrying multiple substitutions in the overlapping C-ter BBXB motifs required for abrogating HS-binding of this isoform.

The relative amounts of each mRNA isoform in *Cxcl12*<sup>Gagtm/Gagtm</sup> were comparable to that of WT littermates (Figure 1C and S2(C)) while serum CXCL12 levels were markedly increased in mutant animals, likely as a consequence of the mutant chemokines to immobilise on HS structures (Figure 1D). Expression and functional analysis of *Cxcl12*<sup>Gagtm/Gagtm</sup> cDNA isoforms confirmed their preserved CXCR4-agonist capacities (Figure S3(D)).

*Cxcl12*<sup>Gagtm/Gagtm</sup> mice were both viable and fertile. Extensive macroscopic and histologic analysis did not reveal any detectable anatomic abnormalities in the *Cxcl12*<sup>Gagtm/Gagtm</sup> mice. Micro photos corresponding to tissue preparations of WT and *Cxcl12*<sup>Gagtm/Gagtm</sup> BM and cerebellum, which development is affected in *Cxcl12* and *Cxcr4* knock-out animals, as well as skeletal muscle, are shown in Figure 1B.

No significant differences in the composition of blood, BM and CD34+ HPC were observed between WT and mutant animals (data not shown). Interestingly, whereas the number of BM haematopoietic cell subpopulations was similar in WT and *Cxcl12*<sup>Gagtm/Gagtm</sup> mice, mutant animals displayed higher numbers of circulating total leukocytes, granulocytes and CD34+

cells (Figure 1E) and no significant differences for both T and B lymphocytes. The number of erythrocytes ( $10.72\pm 0.33/\text{mm}^3$  versus  $10.32\pm 0.31/\text{mm}^3$ ,  $n=6$ ) and that of platelets ( $944\pm 132/\text{mm}^3$  versus  $1029\pm 197/\text{mm}^3$ ,  $n=6$ ) in WT and *Cxcl12*<sup>Gagtm/Gagtm</sup> mice, respectively, were similar.

CXCL12 regulates both the tissue homing and survival of circulating tissue-specific progenitors, HPC and BM-stromal stem cells<sup>32 35</sup>, triggers inflammatory cells infiltration and is required for the peri-endothelial retention of circulating, BM-derived myeloid cells<sup>36 32 35</sup>. These findings prompted us to assess the role of CXCL12/GAG interactions in the regenerative process following acute regional ischemia.

We observed that in both WT and *Cxcl12*<sup>Gagtm/Gagtm</sup> mice, hindlimb-ischemia induced massive transcription and expression of *Cxcl12* isoforms (Figure 2A). Kinetic analysis of mRNA levels showed that *Cxcl12* isoforms expression enhanced by day 4 post-ischemia and returned to basal levels by day 21 (Figure 2A). The expression ratio between the *Cxcl12* isoforms varies between different tissues (Figure S2(D)). Of interest, CXCL12 $\gamma$  was the most abundant isoform in both the normal and ischemic muscle (Figure 2B). We also determined that CXCL12 was expressed in ischemic capillary structure and, in both WT and *Cxcl12*<sup>Gagtm/Gagtm</sup> mice, is co-localized with isolectin B4 staining, a specific marker of endothelial cells (Figure 2C). In addition, CXCL12 expression was also detected in number of arterioles, as revealed by the co-staining between CXCL12 and alpha-smooth muscle actin (Figure 2D).

It is of note that *Cxcl12*<sup>Gagtm/Gagtm</sup> mice displayed a markedly impaired capacity to support efficient post-ischemic revascularization in a model of hindlimb ischemia. Indeed, laser Doppler imaging showed a reduced paw perfusion in ischemic hind limb of *Cxcl12*<sup>Gagtm/Gagtm</sup> as compared to WT animals, as early as day 14 after the onset of ischemia (Figure 3A). Angiographic scores obtained by microangiographic analysis revealed that vessel density was hampered by 30% in ischemic muscle of *Cxcl12*<sup>Gagtm/Gagtm</sup> mice in reference to that of WT

animals (Figure 3B). Furthermore, analysis of post-ischemic frozen calf muscle samples showed that regeneration of both capillary and arteriole vessels were reduced in *Cxcl12<sup>Gagtm/Gagtm</sup>* animals by up to 44% and 55%, respectively as compared to WT animals (Figure 3C and 3D).

As previously mentioned, CXCL12/CXCR4 interactions are involved in the recruitment and/or the retention of circulating cells in the ischemic tissue. To gain further insights into the cellular and molecular mechanisms associated with the reduction of post-ischemic vessel growth in *Cxcl12<sup>Gagtm/Gagtm</sup>* mice, we analyzed the ability of circulating cells to home to ischemic tissues in *Cxcl12<sup>Gagtm/Gagtm</sup>* animals. CD45.1-positive cells were intravenously injected one day after the onset of ischemia, and their number and fate were analysed in the blood and in the ischemic tissue, 6 days after ischemia, a time point associated with a marked upregulation of transcription and expression of *Cxcl12* isoforms. The number of CD45.1+, CD45.1+/CD34+ and CD45.1+/CXCR4+ was higher in the blood of *Cxcl12<sup>Gagtm/Gagtm</sup>* animals compared to that of WT mice. In contrast, the percentage of CD45.1+/CD34+ and CD45.1+/CXCR4+ was decreased in the ischemic muscle of *Cxcl12<sup>Gagtm/Gagtm</sup>* animals compared to that of WT mice (Figure 4A, B). As a consequence, the post-ischemic inflammatory response, a key component of ischemic tissue remodelling is affected in our experimental conditions and we showed that the number of Mac3-positive cells was reduced in ischemic leg of *Cxcl12<sup>Gagtm/Gagtm</sup>* mice compared to WT littermates (Figure 4C).

The predominant expression of CXCL12 $\gamma$  in muscle and in particular its massive accumulation in ischemic tissues, suggests that this isoform might play a critical role in neovascularisation through an HS-binding dependent mechanism. Thus, if the angiogenic defect observed in *Cxcl12<sup>Gagtm/Gagtm</sup>* was due to the selective invalidation of HS-binding capacity of *Cxcl12* products, exogenous administration of wild type CXCL12 proteins with

full HS-binding activity, should restore vascular regeneration in ischemic tissues with the highest efficiency as compared.

To assess this hypothesis we first compared the capacity of both WT CXCL12 $\alpha$  and CXCL12 $\gamma$ , which differ notably for their affinity capacity to bind cell surface in a GAG-dependent manner, to induce post-ischemic vascular regeneration in control animals. Electrotransferred expression of DNA plasmids encoding for CXCL12 $\alpha$  or CXCL12 $\gamma$  (Figure 5A), revealed a dramatically increased potency of CXCL12 $\gamma$  to promote neovascularisation as evaluated by tissue perfusion, angiographic score, capillary density and attraction of inflammatory macrophages in the ischemic tissue (Figure 5B, 5C, 5D and 5E). To bring direct and formal evidence that the superior efficiency of CXCL12 $\gamma$  was actually related to the interaction of the chemokine with HS, we evaluated the pro-angiogenic capacities of CXCL12 $\gamma$  and mutant CXCL12 $\gamma$ m2 which carries the K24S and K27S substitutions combined with the neutralisation of nine of the seventeen positively charged residues encompassed in the C-ter domain of this isoform<sup>12 13</sup> (Figure S3(A)). CXCL12 $\gamma$ m2 displays no detectable HS-binding to cell surface HS whereas it activates CXCR4 with preserved efficiency and even with increased potency as compared to the WT control (Figure S3 (B,C)) and as we reported previously<sup>13</sup>. Our findings unambiguously proved that while CXCL12 $\alpha$  and CXCL12 $\gamma$  showed pro-angiogenic efficiency correlating with their affinities for HS, CXCL12 $\gamma$ m2 failed to induce post-ischemic vessel growth beyond baseline levels (Figure 5B, C and E).

To further investigate the mechanism of the increased pro-angiogenic effect of CXCL12 $\gamma$ , we compared the capacity of each isoform to regulate both the number of cells infiltrating the ischemic tissue and their fate. To this aim, hindlimb ischemia was induced in mice that has been lethally irradiated and reconstituted with BM-derived cells isolated from GFP+ mice. Electrotransfer of CXCL12 $\gamma$  plasmid enhanced by 300% and 150% the number of GFP+ cells

infiltrating the ischemic muscle compared to mice treated with empty plasmid or CXCL12 $\alpha$ , respectively (Figure 6A). The failure of CXCL12 $\gamma$ m2 to induce a significant effect further proved the involvement of an HS-dependent mechanism in the robust neovascularisation induced by CXCL12 $\gamma$ . Of note, the percentage of GFP<sup>+</sup>/BS1-lectin<sup>+</sup> cells of the endothelial lineage, and that of GFP<sup>+</sup>/Mac3<sup>+</sup> revealing the macrophage phenotype, were similar in mice treated with CXCL12 $\gamma$  or CXCL12 $\alpha$ . Further experiments using human endothelial progenitor cells (EPC) labelled with CFSE revealed that CXCL12 $\gamma$ , but not CXCL12 $\gamma$ m2, increased the number of EPC infiltrating ischemic hindlimb muscle (day 4 post-ischemia) by 150% and subsequently vessel growth by roughly 50% (day 14 post-ischemia) when compared to mice treated with CXCL12 $\alpha$  (Figure S4).

Collectively, these results suggest that CXCL12 $\gamma$  regulates the accumulation of BM-derived cells in ischemic tissues with the highest efficiency, in comparison to CXCL12 $\alpha$ , and in a strictly HS-dependent manner, while it does not differ from CXCL12 $\alpha$  regarding induction of cell differentiation. The increased number of EPC homing to the injured muscle early after ischemia permits to ascribe its prominent pro-angiogenic effect to a primary attraction of endothelial cell precursors.

Finally, to demonstrate that the deficient neoangiogenesis observed in *Cxcl12*<sup>Gagtm/Gagtm</sup> animals was related to the expression of CXCL12 HS-binding mutants and their inability to promote efficient vascular reparation, we electrotransferred a plasmid encoding WT CXCL12 $\gamma$  plasmid in the ischemic hindlimb. Expression of this isoform virtually normalized vascular regeneration in ischemic tissues as proved by the significant increase in both vessel density and infiltration of inflammatory macrophages (Figure 7). This finding conclusively links the default of tissue reparation observed in these animals to the reduced capacity of mutant CXCL12 proteins to form complexes with HS proteoglycans.

## DISCUSSION

The animal model we have engineered allows the selective characterization of proteoglycan-chemokine interactions *in vivo*, separately from interactions of a defined chemokine to its specific receptor. *Cxcl12<sup>Gagtm/Gagtm</sup>* mice exhibit normal expression of isoform-specific *Cxcl12* mRNAs encoding for CXCR4-agonist chemokines. No detectable developmental anomalies were observed in *Cxcl12<sup>Gagtm/Gagtm</sup>* animals. This is in sharp contrast to *Cxcl12-* and *Cxcr4-* deficient mice, which show in both cases abnormal haematopoiesis and multiple organogenesis default associated to perinatal mortality<sup>20 21 37</sup>, and to *Cxcr7-* knock-out mice, which show disrupted cardiac development<sup>38</sup>. Manifold reasons could explain the lack of detectable anatomic anomalies in the mutant animals. First, the preserved expression levels of total and isoform specific *Cxcl12* mRNA in *Cxcl12<sup>Gagtm/Gagtm</sup>* mice tissues. Second, the intact cell signaling capacities of mutant chemokines leading to orientated cell migration, as previously shown for mutated CCL19 and CCL21<sup>1</sup>. Third, the oligosaccharidic HS structure recognized by CXCL12, which remains unknown, could not feature during embryogenesis the high affinity CXCL12 binding site, thus explaining the lack of observed effects. In this line, it has been proved a binding specificity switch of brain HS proteoglycans from FGF-2 to FGF-1<sup>39</sup>, demonstrating that indeed the binding capacity of embryonic HS for a given protein is not necessarily present, and is acquired during development.

The *Cxcl12<sup>Gagtm/Gagtm</sup>* mice nevertheless display a subtle anomaly revealing an increased number of circulating white blood cells, including CD34+ HPC. This phenomenon could be explained by a reduced attraction/retention in lymphoid tissues and is probably related to impaired HS-dependent tissue adhesiveness of the CXCL12 mutant proteins<sup>15 5</sup>. Given the crucial role played by CXCL12 and CXCR4 in both the homing of haematopoietic cells to the BM<sup>25 26</sup>, the inability of the HS-binding CXCL12 mutants to adhere to the cell surface and the surrounding extracellular matrix of CXCL12-producing stromal cells, forming CXCL12-BM

niches<sup>40</sup> could facilitate their egress from the BM. In this regard, the accumulation of circulating CD34<sup>+</sup> cells, which normally reside in BM<sup>41</sup>, strongly argues in favour of reduced retention of these cells in BM. The BM egress of the mature leukocytes could also be due to the same mechanism. Alternatively, the increased number of these cells in the periphery could be ascribed to the gradient generated by the blood accumulation of free, HS-binding disabled CXCL12 proteins and/or their failure to firmly immobilize on the apical surface of sinus and post-capillary endothelial cells<sup>13 15</sup> that would inhibit the return of leukocytes to the BM<sup>42</sup>.

Whereas basal coronary flow were impaired in *Cxcr4*(+/-) mice, paralleled by reduced angiogenesis and myocardial vessel density, we did not detect changes in the basal number of capillary and arterioles in skeletal muscle of *Cxcl12*<sup>Gagtm/Gagtm</sup> animals<sup>43</sup>. In contrast, *Cxcl12*<sup>Gagtm/Gagtm</sup> animals show a marked default in angiogenesis and neovascularisation of ischemic tissues, revealing a biological role for CXCL12/GAG interactions in tissue repair after ischemia. It has been previously reported that recruitment of CXCR4-positive progenitor cells to regenerating tissues is mediated by hypoxic gradients *via* HIF-1-induced expression of CXCL12<sup>32</sup>. Furthermore, CXCL12 attracts EPC, induces angiogenesis and increases the number of newly formed vessels and blood flow in models of hindlimb ischemia when overexpressed, either alone<sup>44</sup> or combined with cell therapy<sup>45</sup>. Recruitment and retention of BM-derived circulating inflammatory cells mediated by CXCL12 participates to vascular remodelling and arteriole growth<sup>36</sup>. In addition, CXCL12 seems to have a direct effect on migration of smooth muscle cells and smooth muscle progenitor cells<sup>46</sup>.

However, all previous studies focussed on deciphering the capacity of CXCL12 $\alpha$  to promote angiogenesis, without dissecting the respective contribution of receptor activation and GAG-binding. Furthermore, only the therapeutic capacity of exogenous WT chemokines was investigated, while the role played by endogenous CXCL12/GAG interactions in the spontaneous post-ischemic recovery remained unknown.

The defective post-ischemic neovascularisation observed in *Cxcl12*<sup>Gagtm/Gagtm</sup> animals thus brings a new light to the original evidence that, beyond CXCL12-induced receptor cell signalling, the endogenous CXCL12/GAG interactions play a critical role in tissue regeneration and in particular in vascular growth. Indeed, the efficiency of CXCL12 $\gamma$  to rescue the default in *Cxcl12*<sup>Gagtm/Gagtm</sup> animals contrasts with the lack of effect of CXCL12 $\gamma$ m2 and reveals the key role of this mechanism in the reparative process. This finding is in keeping with the efficiency of CXCL12 $\gamma$  and the inability of CXCL12 $\gamma$ m2 to promote homing of BM-derived circulating inflammatory cells and of circulating EPC into ischemic tissues, and modulate vessel growth in this setting.

Bound to HS-structures on the apical surface of endothelial cells<sup>47</sup>, CXCL12 expressed by autocrine or juxtacrine mechanisms could be determinant for vascular targeting of circulating progenitor and inflammatory cells and induction, in an integrin- and CXCR4-dependent manner, of both firm adhesion and transendothelial migration of infiltrating BM-derived cells<sup>48</sup>. Among CXCL12 isoforms, CXCL12 $\gamma$  binds to microvascular endothelial cell surface with the highest efficiency<sup>13 47</sup> and is ideally suited to accomplish this role. Abundantly expressed and induced in injured tissues by hypoxia, CXCL12 $\gamma$  could delimit a static field of chemokine keeping cells motile (haptokinesis) in a restrained tissue compartment. This may contribute to the reparative effect of EPC by enhancing cell-adhesiveness and survival<sup>49</sup>. It could be hypothesized that, released progressively upon cleavage of its C-ter domain the pool of immobilized CXCL12 $\gamma$  could provide a gradient of active, diffusible chemokines that would promote long-range chemotaxis toward the injured tissue. An analogous mechanism contributes to the regulation by CCL21 of lymphocyte T cell homing in secondary lymphoid organs<sup>1</sup>.

Regarding the potential of CXCL12 in regenerative medicine, the continuous delivery or administration in an immobilized form of CXCL12 $\alpha$  is required to provide therapeutic effect

in post-ischemic treatment<sup>50</sup>. CXCL12 $\gamma$  could overcome this limitation thus activating efficiently the pro-angiogenic mechanisms.

Collectively, our findings unravel the contribution of endogenous CXCL12/HS complexes to the biological functions of this chemokine. The prevalence of CXCL12 $\gamma$  expression in hypoxic conditions and its superior capacity to promote neovascularisation further highlights the importance of HS-binding mechanisms in the tissue reparative activity of CXCL12.

The findings of this work pave the way for investigating the contribution of CXCL12/HS interactions to other homeostatic and physio-pathological functions played by this unique chemokine and could have broad relevance eventually for other chemokine systems.

## **FUNDING SOURCES**

This work was supported by grants from Agence Nationale de la Recherche (ANR; Chemoglycan, NT05-4\_41967; Chemrepair 2010-BLAN112702), INSERM, Institut Pasteur PTR-395, Mizutani Foundation (Japan) and by institutional funding from INSERM. J.S.S is a recipient of a Contrat d'Interface from Assistance Publique-Hôpitaux de Paris and supported by "Fondation pour la Recherche Médicale". P.R and P.G are recipients of ANR fellowships. A.Récalde is a recipient of fellowships from Fondation pour la Recherche Médicale and from Région Ile de France. The Funders had no role in study design, data collection and analysis, decision to publish, or preparation of the manuscript.

## **DISCLOSURES**

None

## REFERENCES

1. Schumann K, Lammermann T, Bruckner M, Legler DF, Polleux J, Spatz JP, Schuler G, Forster R, Lutz MB, Sorokin L, Sixt M. Immobilized chemokine fields and soluble chemokine gradients cooperatively shape migration patterns of dendritic cells. *Immunity*. 2010;32:703-713
2. Campbell JJ, Hedrick J, Zlotnik A, Siani MA, Thompson DA, Butcher EC. Chemokines and the arrest of lymphocytes rolling under flow conditions. *Science*. 1998;279:381-384
3. Lortat-Jacob H. The molecular basis and functional implications of chemokine interactions with heparan sulphate. *Curr Opin Struct Biol*. 2009;19:543-548
4. Lortat-Jacob H, Grosdidier A, Imberty A. Structural diversity of heparan sulfate binding domains in chemokines. *Proc Natl Acad Sci U S A*. 2002;99:1229-1234
5. Sweeney EA, Lortat-Jacob H, Priestley GV, Nakamoto B, Papayannopoulou T. Sulfated polysaccharides increase plasma levels of sdf-1 in monkeys and mice: Involvement in mobilization of stem/progenitor cells. *Blood*. 2002;99:44-51
6. Bao X, Moseman EA, Saito H, Petryniak B, Thiriot A, Hatakeyama S, Ito Y, Kawashima H, Yamaguchi Y, Lowe JB, von Andrian UH, Fukuda M. Endothelial heparan sulfate controls chemokine presentation in recruitment of lymphocytes and dendritic cells to lymph nodes. *Immunity*. 2010;33:817-829
7. Proudfoot AE, Handel TM, Johnson Z, Lau EK, LiWang P, Clark-Lewis I, Borlat F, Wells TN, Kosco-Vilbois MH. Glycosaminoglycan binding and oligomerization are essential for the in vivo activity of certain chemokines. *Proc Natl Acad Sci U S A*. 2003;100:1885-1890

8. Laguri C, Arenzana-Seisdedos F, Lortat-Jacob H. Relationships between glycosaminoglycan and receptor binding sites in chemokines-the cxcl12 example. *Carbohydr Res.* 2008;343:2018-2023
9. Tashiro K, Tada H, Heilker R, Shirozu M, Nakano T, Honjo T. Signal sequence trap: A cloning strategy for secreted proteins and type i membrane proteins. *Science.* 1993;261:600-603
10. Gleichmann M, Gillen C, Czardybon M, Bosse F, Greiner-Petter R, Auer J, Muller HW. Cloning and characterization of sdf-1gamma, a novel sdf-1 chemokine transcript with developmentally regulated expression in the nervous system. *Eur J Neurosci.* 2000;12:1857-1866
11. Amara A, Lorthioir O, Valenzuela A, Magerus A, Thelen M, Montes M, Virelizier JL, Delepierre M, Baleux F, Lortat-Jacob H, Arenzana-Seisdedos F. Stromal cell-derived factor-1alpha associates with heparan sulfates through the first beta-strand of the chemokine. *J Biol Chem.* 1999;274:23916-23925
12. Laguri C, Sadir R, Rueda P, Baleux F, Gans P. The novel cxcl12c isoform encodes an unstructured cationic domain which regulates bioactivity and interaction with both glycosaminoglycans and cxcr4. *PLoS ONE* 2007;2:e111
13. Rueda P, Balabanian K, Lagane B, Staropoli I, Chow K, Levoye A, Laguri C, Sadir R, Delaunay T, Izquierdo E, Pablos JL, Lendinez E, Caruz A, Franco D, Baleux F, Lortat-Jacob H, Arenzana-Seisdedos F. The cxcl12gamma chemokine displays unprecedented structural and functional properties that make it a paradigm of chemoattractant proteins. *PLoS One.* 2008;3:e2543

14. Sadir R, Baleux F, Grosdidier A, Imberty A, Lortat-Jacob H. Characterization of the stromal cell-derived factor-1alpha-heparin complex. *J Biol Chem.* 2001;276:8288-8296
15. O'Boyle G, Mellor P, Kirby JA, Ali S. Anti-inflammatory therapy by intravenous delivery of non-heparan sulfate-binding cxcl12. *Faseb J.* 2009;23:3906-3916
16. Oberlin E, Amara A, Bachelier F, Bessia C, Virelizier JL, Arenzana-Seisdedos F, Schwartz O, Heard JM, Clark-Lewis I, Legler DF, Loetscher M, Baggiolini M, Moser B. The cxc chemokine sdf-1 is the ligand for lestr/fusin and prevents infection by t-cell-line-adapted hiv-1. *Nature.* 1996;382:833-835
17. Bleul CC, Farzan M, Choe H, Parolin C, Clark-Lewis I, Sodroski J, Springer TA. The lymphocyte chemoattractant sdf-1 is a ligand for lestr/fusin and blocks hiv-1 entry. *Nature.* 1996;382:829-833
18. Balabanian K, Lagane B, Infantino S, Chow KY, Harriague J, Moepps B, Arenzana-Seisdedos F, Thelen M, Bachelier F. The chemokine sdf-1/cxcl12 binds to and signals through the orphan receptor rdc1 in t lymphocytes. *J Biol Chem.* 2005;280:35760-35766
19. Burns JM, Summers BC, Wang Y, Melikian A, Berahovich R, Miao Z, Penfold ME, Sunshine MJ, Littman DR, Kuo CJ, Wei K, McMaster BE, Wright K, Howard MC, Schall TJ. A novel chemokine receptor for sdf-1 and i-tac involved in cell survival, cell adhesion, and tumor development. *J Exp Med.* 2006;203:2201-2213
20. Nagasawa T, Hirota S, Tachibana K, Takakura N, Nishikawa S, Kitamura Y, Yoshida N, Kikutani H, Kishimoto T. Defects of b-cell lymphopoiesis and bone-marrow myelopoiesis in mice lacking the cxc chemokine pbsf/sdf-1. *Nature.* 1996;382:635-638

21. Ma Q, Jones D, Borghesani PR, Segal RA, Nagasawa T, Kishimoto T, Bronson RT, Springer TA. Impaired b-lymphopoiesis, myelopoiesis, and derailed cerebellar neuron migration in *cxcr4*- and *sdf-1*-deficient mice. *Proc Natl Acad Sci U S A*. 1998;95:9448-9453
22. Coulomb-L'Hermin A, Amara A, Schiff C, Durand-Gasselini I, Foussat A, Delaunay T, Chaouat G, Capron F, Ledee N, Galanaud P, Arenzana-Seisdedos F, Emilie D. Stromal cell-derived factor 1 (*sdf-1*) and antenatal human b cell lymphopoiesis: Expression of *sdf-1* by mesothelial cells and biliary ductal plate epithelial cells. *Proc Natl Acad Sci U S A*. 1999;96:8585-8590
23. Pablos JL, Amara A, Bouloc A, Santiago B, Caruz A, Galindo M, Delaunay T, Virelizier JL, Arenzana-Seisdedos F. Stromal-cell derived factor is expressed by dendritic cells and endothelium in human skin. *Am J Pathol*. 1999;155:1577-1586
24. Aiuti A, Webb IJ, Bleul C, Springer T, Gutierrez-Ramos JC. The chemokine *sdf-1* is a chemoattractant for human *cd34+* hematopoietic progenitor cells and provides a new mechanism to explain the mobilization of *cd34+* progenitors to peripheral blood. *J Exp Med*. 1997;185:111-120
25. Petit I, Szyper-Kravitz M, Nagler A, Lahav M, Peled A, Habler L, Ponomaryov T, Taichman RS, Arenzana-Seisdedos F, Fujii N, Sandbank J, Zipori D, Lapidot T. G-CSF induces stem cell mobilization by decreasing bone marrow *sdf-1* and up-regulating *cxcr4*. *Nat Immunol*. 2002;3:687-694
26. Broxmeyer HE, Kohli L, Kim CH, Lee Y, Mantel C, Cooper S, Hangoc G, Shaheen M, Li X, Clapp DW. Stromal cell-derived factor-1/*cxcl12* directly enhances survival/antiapoptosis of myeloid progenitor cells through *cxcr4* and *g(alpha)i* proteins and enhances engraftment of competitive, repopulating stem cells. *J Leukoc Biol*. 2003;73:630-638

27. Peled A, Grabovsky V, Habler L, Sandbank J, Arenzana-Seisdedos F, Petit I, Ben-Hur H, Lapidot T, Alon R. The chemokine sdf-1 stimulates integrin-mediated arrest of cd34(+) cells on vascular endothelium under shear flow. *J Clin Invest.* 1999;104:1199-1211
28. Okada T, Ngo VN, Ekland EH, Forster R, Lipp M, Littman DR, Cyster JG. Chemokine requirements for b cell entry to lymph nodes and peyer's patches. *J Exp Med.* 2002;196:65-75
29. Scimone ML, Felbinger TW, Mazo IB, Stein JV, Von Andrian UH, Weninger W. Cxcl12 mediates ccr7-independent homing of central memory cells, but not naive t cells, in peripheral lymph nodes. *J Exp Med.* 2004;199:1113-1120
30. Kryczek I, Wei S, Keller E, Liu R, Zou W. Stroma-derived factor (sdf-1/cxcl12) and human tumor pathogenesis. *Am J Physiol Cell Physiol.* 2007;292:C987-995
31. Pablos JL, Santiago B, Galindo M, Torres C, Brehmer MT, Blanco FJ, Garcia-Lazaro FJ. Synoviocyte-derived cxcl12 is displayed on endothelium and induces angiogenesis in rheumatoid arthritis. *J Immunol.* 2003;170:2147-2152
32. Ceradini DJ, Kulkarni AR, Callaghan MJ, Tepper OM, Bastidas N, Kleinman ME, Capla JM, Galiano RD, Levine JP, Gurtner GC. Progenitor cell trafficking is regulated by hypoxic gradients through hif-1 induction of sdf-1. *Nat Med.* 2004;10:858-864
33. Foubert P, Silvestre JS, Souttou B, Barateau V, Martin C, Ebrahimian TG, Lere-Dean C, Contreres JO, Sulpice E, Levy BI, Plouet J, Tobelem G, Le Ricousse-Roussanne S. Psgl-1-mediated activation of ephb4 increases the proangiogenic potential of endothelial progenitor cells. *J Clin Invest.* 2007;117:1527-1537
34. Silvestre JS, Thery C, Hamard G, Boddaert J, Aguilar B, Delcayre A, Houbron C, Tamarat R, Blanc-Brude O, Heeneman S, Clergue M, Duriez M, Merval R, Levy B,

- Tedgui A, Amigorena S, Mallat Z. Lactadherin promotes vegf-dependent neovascularization. *Nat Med.* 2005;11:499-506
35. Cashman J, Clark-Lewis I, Eaves A, Eaves C. Stromal-derived factor 1 inhibits the cycling of very primitive human hematopoietic cells in vitro and in nod/scid mice. *Blood.* 2002;99:792-799
36. Grunewald M, Avraham I, Dor Y, Bachar-Lustig E, Itin A, Jung S, Chimenti S, Landsman L, Abramovitch R, Keshet E. Vegf-induced adult neovascularization: Recruitment, retention, and role of accessory cells. *Cell.* 2006;124:175-189
37. Zou YR, Kottmann AH, Kuroda M, Taniuchi I, Littman DR. Function of the chemokine receptor cxcr4 in haematopoiesis and in cerebellar development. *Nature.* 1998;393:595-599
38. Sierro F, Biben C, Martinez-Munoz L, Mellado M, Ransohoff RM, Li M, Woehl B, Leung H, Groom J, Batten M, Harvey RP, Martinez AC, Mackay CR, Mackay F. Disrupted cardiac development but normal hematopoiesis in mice deficient in the second cxcl12/sdf-1 receptor, cxcr7. *Proc Natl Acad Sci U S A.* 2007;104:14759-14764
39. Nurcombe V, Ford MD, Wildschut JA, Bartlett PF. Developmental regulation of neural response to fgf-1 and fgf-2 by heparan sulfate proteoglycan. *Science.* 1993;260:103-106
40. Sugiyama T, Kohara H, Noda M, Nagasawa T. Maintenance of the hematopoietic stem cell pool by cxcl12-cxcr4 chemokine signaling in bone marrow stromal cell niches. *Immunity.* 2006;25:977-988
41. Levesque JP, Winkler IG. Mobilization of hematopoietic stem cells: State of the art. *Curr Opin Organ Transplant.* 2008;13:53-58

42. Martin C, Burdon PC, Bridger G, Gutierrez-Ramos JC, Williams TJ, Rankin SM. Chemokines acting via cxcr2 and cxcr4 control the release of neutrophils from the bone marrow and their return following senescence. *Immunity*. 2003;19:583-593
43. Liehn EA, Tuchscheerer N, Kanzler I, Drechsler M, Fraemohs L, Schuh A, Koenen RR, Zander S, Soehnlein O, Hristov M, Grigorescu G, Urs AO, Leabu M, Bucur I, Merx MW, Zernecke A, Ehling J, Gremse F, Lammers T, Kiessling F, Bernhagen J, Schober A, Weber C. Double-edged role of the cxcl12/cxcr4 axis in experimental myocardial infarction. *J Am Coll Cardiol*. 2011;58:2415-2423
44. Hiasa K, Ishibashi M, Ohtani K, Inoue S, Zhao Q, Kitamoto S, Sata M, Ichiki T, Takeshita A, Egashira K. Gene transfer of stromal cell-derived factor-1alpha enhances ischemic vasculogenesis and angiogenesis via vascular endothelial growth factor/endothelial nitric oxide synthase-related pathway: Next-generation chemokine therapy for therapeutic neovascularization. *Circulation*. 2004;109:2454-2461
45. Yamaguchi J, Kusano KF, Masuo O, Kawamoto A, Silver M, Murasawa S, Bosch-Marce M, Masuda H, Losordo DW, Isner JM, Asahara T. Stromal cell-derived factor-1 effects on ex vivo expanded endothelial progenitor cell recruitment for ischemic neovascularization. *Circulation*. 2003;107:1322-1328
46. Zernecke A, Schober A, Bot I, von Hundelshausen P, Liehn EA, Mopps B, Mericskay M, Gierschik P, Biessen EA, Weber C. Sdf-1alpha/cxcr4 axis is instrumental in neointimal hyperplasia and recruitment of smooth muscle progenitor cells. *Circ Res*. 2005;96:784-791
47. Santiago B, Izquierdo E, Rueda P, Del Rey MJ, Criado G, Usategui A, Arenzana-Seisdedos F, Pablos JL. Cxcl12gamma isoform is expressed on endothelial and dendritic cells in rheumatoid arthritis synovium and regulates t cell activation. *Arthritis Rheum*. 2012;64:409-417

48. Shamri R, Grabovsky V, Gauguet JM, Feigelson S, Manevich E, Kolanus W, Robinson MK, Staunton DE, von Andrian UH, Alon R. Lymphocyte arrest requires instantaneous induction of an extended lfa-1 conformation mediated by endothelium-bound chemokines. *Nat Immunol.* 2005;6:497-506
49. Avraamides CJ, Garmy-Susini B, Varner JA. Integrins in angiogenesis and lymphangiogenesis. *Nat Rev Cancer.* 2008;8:604-617
50. Segers VF, Revin V, Wu W, Qiu H, Yan Z, Lee RT, Sandrasagra A. Protease-resistant stromal cell-derived factor-1 for the treatment of experimental peripheral artery disease. *Circulation.* 2011;123:1306-1315

## FIGURE LEGENDS

**Figure 1. Characterization of *Cxcl12*<sup>Gagtm/Gagtm</sup> mice.** (A) Schematic representation of *Cxcl12* genomic locus, targeting vector and recombined *Cxcl12* locus (*Cxcl12*<sup>Gagtm</sup>). Exons 1-4 are represented by darked boxes. Mutations incorporating residue substitutions (2<sup>nd</sup> exon) and stop codon (4<sup>th</sup> exon) are indicated by vertical arrows and stars. The LoxP-FRT-Neo cassette is inserted in an opposite orientation regarding to the target gene in intron 3-4. Long (LA) and short (SA) homology arm positions and length are indicated. (B) Hematoxylin and eosin staining of bone marrow (left panels), cerebellum (middle panels) and skeletal muscle (right panels) tissue sections from *Cxcl12*<sup>Gagtm/Gagtm</sup> (MUT) and wild-type littermate (WT) animals. Arrows show megakaryocytes; 1 display white substance; 2, granular layer; 3, molecular layer. (C) Real-time PCR analysis of *Cxcl12*. Relative RNA expression levels of *Cxcl12* isoforms normalized to HPRT in cerebellum, bone marrow and skeletal muscle tissues. *Cxcl12* $\alpha$ , *Cxcl12* $\beta$  and *Cxcl12* $\gamma$  ARN levels on MUT animals are expressed relative to the WT animals level, arbitrary set to 1 (n=12 per group). (D). CXCL12 levels in blood were measured by ELISA in MUT and WT animals. (E) Cell populations in peripheral blood collected from MUT and WT animals. Results are mean $\pm$ SEM. \*\*p<0.01, \*\*\*p<0.001 versus WT.

**Figure 2. Expression of CXCL12 isoforms in ischemic tissue.** (A) Quantitative evaluation and relative levels of CXCL12 $\alpha$ , CXCL12 $\beta$  and CXCL12 $\gamma$  mRNA contents 1, 4, 6 and 21 days after ischemia in ischemic and non ischemic legs of *Cxcl12*<sup>Gagtm/Gagtm</sup> (MUT) and wild-type littermate (WT) animals. Values are mean  $\pm$  SEM. n=10/group, representative of 2 independent experiments. 28 possible comparisons for Bonferroni correction, a value of p<0.0018 was considered significant, \*\*p<0.0003 versus N Isch at day 1. (B) mRNA levels of each *Cxcl12* isoform were normalized to that of *Cxcl12* $\alpha$  in skeletal muscle of non ischemic

tissue. 6 possible comparisons for Bonferroni correction, a value of  $p < 0.008$  was considered significant,  $n = 10$  per group. (C-D) Histological sections from ischemic skeletal muscles of WT and MUT animals showing CXCL12 expression in capillary (c) and arteriolar (d) structures. Red staining, alpha smooth muscle actin (alpha smooth muscle cells); green staining, Griffonia Simplicifolia Agglutinin isolectin B4 (endothelial cells); purple staining, CXCL12. Nuclei were stained with DAPI (blue staining). Bars:  $10\mu\text{m}$ . One representative experiment out of six is shown.

**Figure 3. Postischemic revascularization in *Cxcl12<sup>Gagtm/Gagtm</sup>* animals. Quantitative evaluation and representative photomicrographs of foot perfusion at different time points (A), and at day 21, for angiographic score (B, vessels in white), capillary density (C, capillaries in green, arrows show fibronectin-labelled capillaries), arteriole density (D, arterioles in green, arrows show  $\alpha$ -actin-labelled arterioles) in *Cxcl12<sup>Gagtm/Gagtm</sup>* (MUT) and wild-type littermate (WT) animals. Results are shown in ischemic (Isc) and non-ischemic (N.Isc) legs. D indicates day. Values are mean  $\pm$  SEM.  $n = 15$  per group, representative of 3 independent experiments. A) 15 possible comparisons for Bonferroni correction, a value of  $p < 0.003$  was considered significant,  $*p < 0.03$  and  $**p < 0.0006$  versus WT. B) 1 possible comparisons for Bonferroni correction, a value of  $p < 0.05$  was considered significant,  $***p < 0.001$  versus WT.  $n = 15$  per group. C-D) 6 possible comparisons for Bonferroni correction, a value of  $p < 0.008$  was considered significant,  $**p < 0.0016$  versus Isc WT.  $n = 15$  per group.**

**Figure 4. Quantification of infiltrating circulating cells in *Cxcl12<sup>Gagtm/Gagtm</sup>* animals. Percentage of CD45.1+, CD45.1+/CD34+ and CD45.1+/CXCR4+ in blood (A) and ischemic muscle (B), 6 days after the onset of ischemia. Representative FACS dot plots obtained from WT and MUT digested muscle at 6 days after ischemia. Cells were gated on CXCR4**

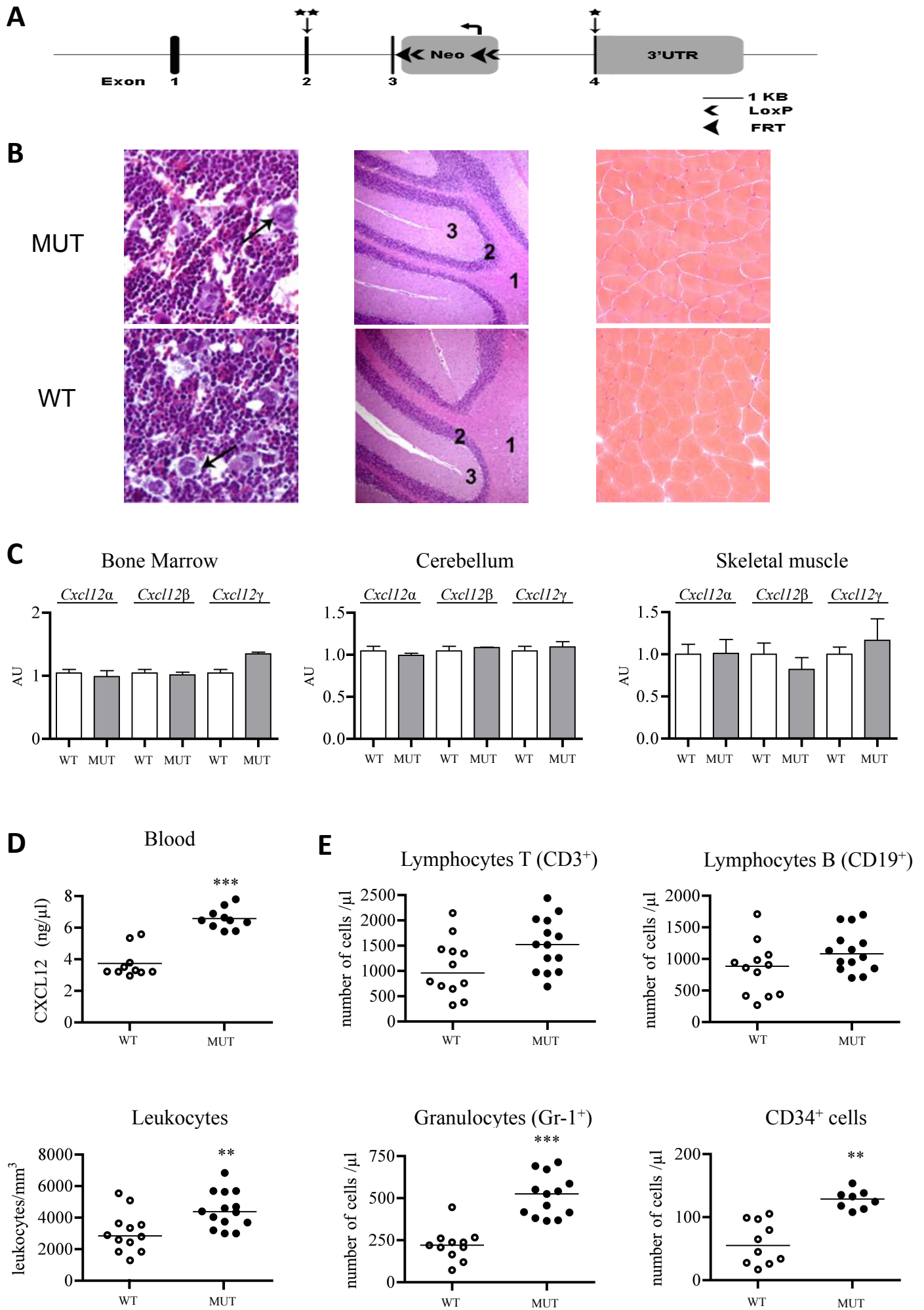
expressing CD45.1-positive cells. n = 7 per group. A-B) 1 possible comparisons for Bonferroni correction, a value of  $p < 0.05$  was considered significant. \* $p < 0.05$  versus WT. (C) Quantitative evaluation and representative photomicrographs of Mac3-positive cells (macrophages in brown, arrows show Mac-3 labelled macrophages) in *Cxcl12*<sup>Gagtm/Gagtm</sup> (MUT) and wild-type littermate (WT) animals. Results are shown in ischemic (Isc) and non-ischemic (N.Isc) legs. Values are mean  $\pm$  SEM. n = 15 per group, representative of 3 independent experiments. 6 possible comparisons for Bonferroni correction, a value of  $p < 0.008$  was considered significant, \*\* $p < 0.0016$  versus Isc WT.

**Figure 5. Effect of CXCL12 isoforms on post-ischemic revascularization.** Quantitative evaluation of foot perfusion (A), microangiography (B), capillary density (C), and arteriolar density (D) and macrophages infiltration (E), 21 days after ischemia in C57BL/6 mice transfected with empty DNA plasmid (CONT) or DNA expression vectors encoding CXCL12 $\alpha$ , CXCL12 $\gamma$  or CXCL12 $\gamma$ m2. Values are mean  $\pm$  SEM. n = 15 per group, representative of 3 independent experiments. A-B) 6 possible comparisons for Bonferroni correction, a value of  $p < 0.008$  was considered significant, \* $p < 0.008$ , \*\* $p < 0.0016$  versus PBS, †  $p < 0.008$  versus CXCL12 $\alpha$ , # $p < 0.008$ , ### $p < 0.0016$  versus CXCL12 $\gamma$ . C-E) 28 possible comparisons for Bonferroni correction, a value of  $p < 0.0017$  was considered significant, \* $p < 0.0017$  versus Isc CONT, † $p < 0.0017$  versus Isc CXCL12 $\alpha$ , # $p < 0.0017$  versus Isc CXCL12 $\gamma$ . Isc indicates ischemic leg and N.Isc, non ischemic leg.

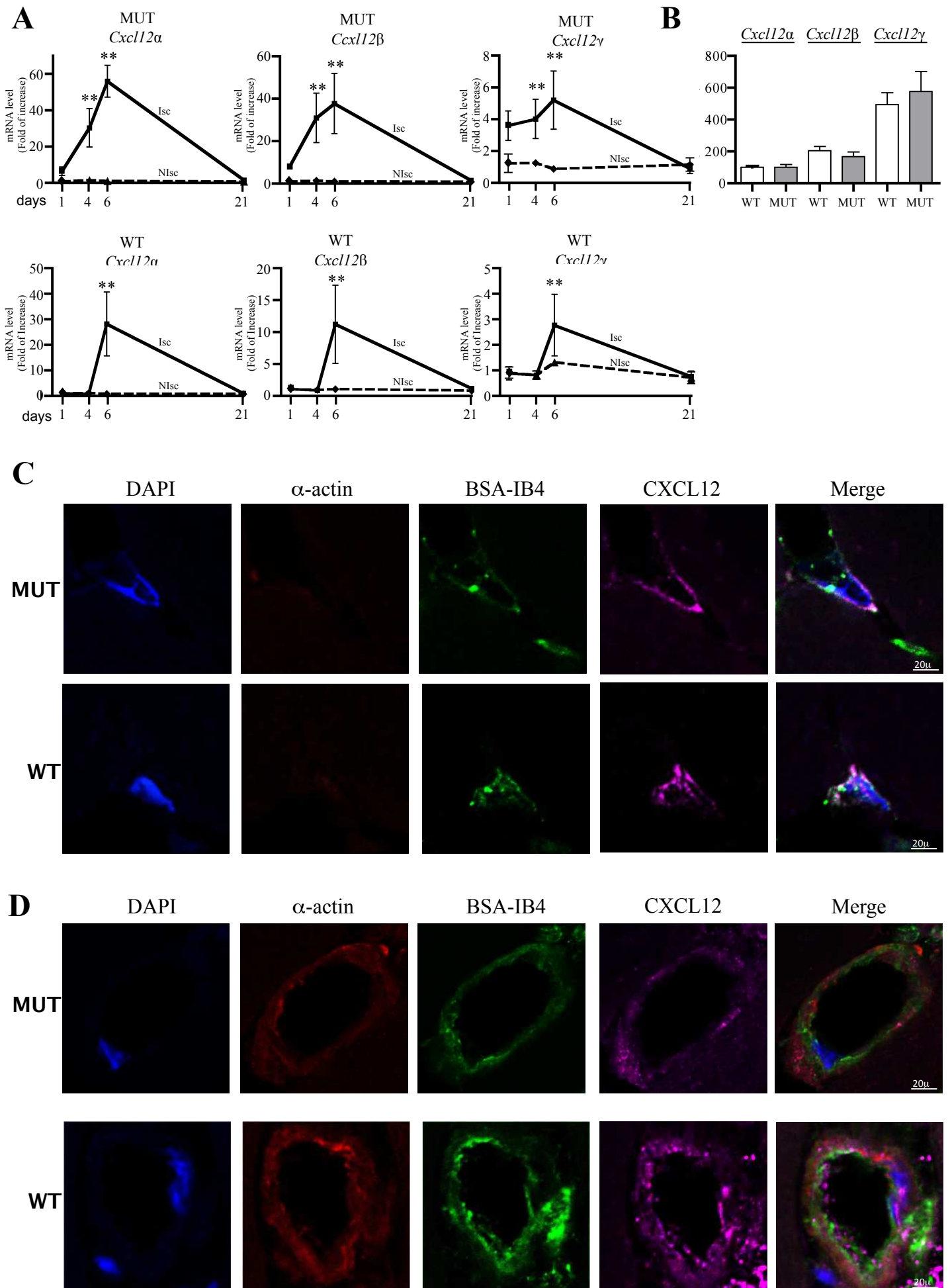
**Figure 6. CXCL12 $\gamma$  controls BM-derived cells infiltration in ischemic tissues.** Quantitative evaluation and representative photomicrographs of the percentage of GFP-expressing cells (A), GFP-expressing and BS1-labelled cells (B) and GFP-expressing and Mac3-labelled cells (C) in the ischemic leg of irradiated wild-type mice reconstituted with

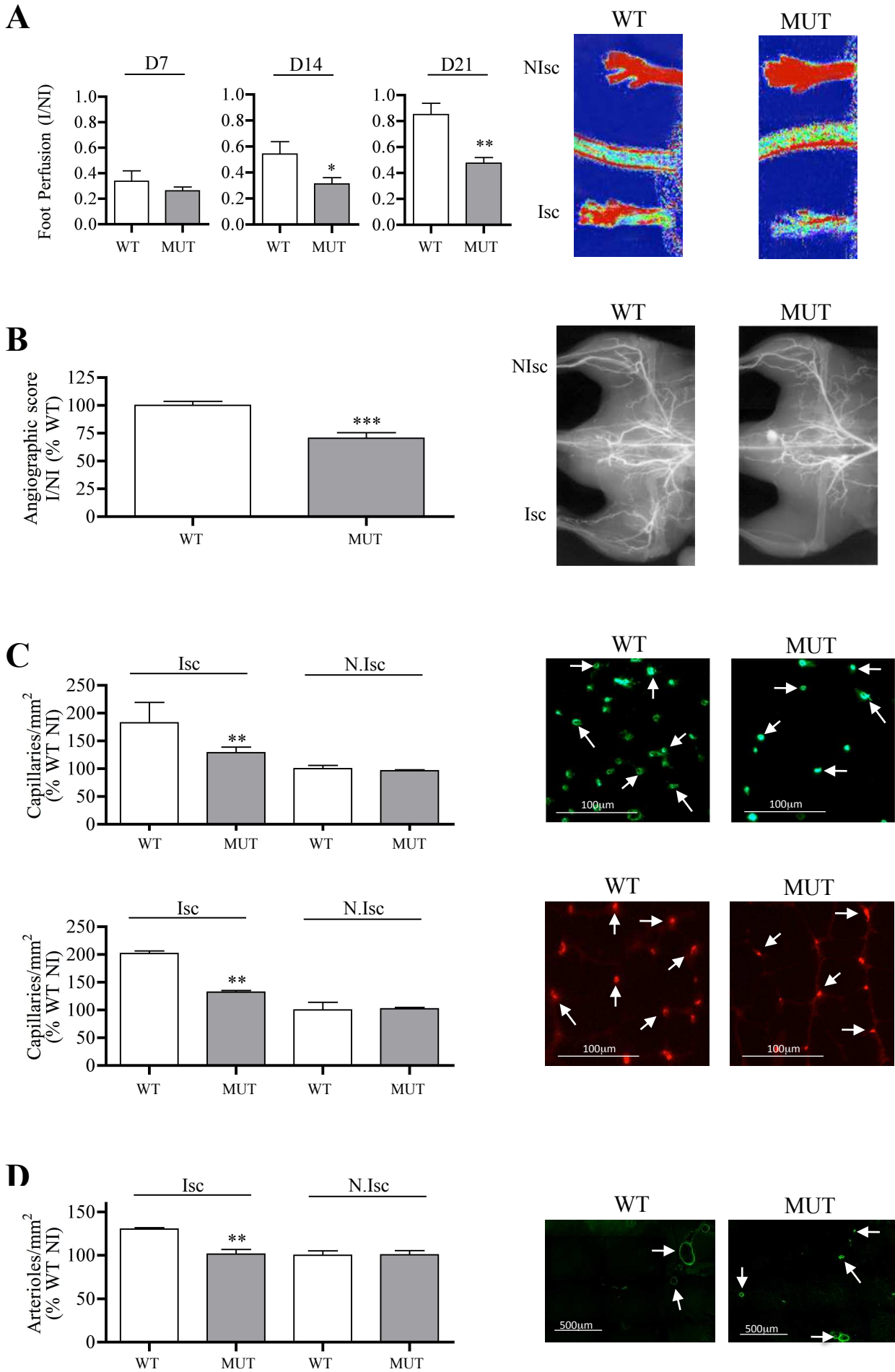
bone marrow of WT GFP+ animals and treated with empty DNA plasmid (CONT), or DNA expression vectors encoding for CXCL12 $\alpha$ , CXCL12 $\gamma$  or HS-binding mutant CXCL12 $\gamma$ m2 . Value quantification are represented in histograms. Values are mean  $\pm$  SEM. n = 10 per group, representative of 2 independent experiments. A-C) 28 possible comparisons for Bonferroni correction, a value of  $p < 0.0017$  was considered significant, \* $p < 0.0017$  versus Isc CONT, † $p < 0.0017$  versus Isc CXCL12 $\alpha$ , # $p < 0.0017$  versus Isc CXCL12 $\gamma$ . Isc indicates ischemic leg and N.Isc, non ischemic leg.

**Figure 7. CXCL12 $\gamma$  restores the defective angiogenic phenotype in *Cxcl12*<sup>Gagtm/Gagtm</sup> animals.** Quantitative evaluation of foot perfusion (A), capillary density (B), arteriole density (C) and Mac3-positive cells (D) in *Cxcl12*<sup>Gagtm/Gagtm</sup> (MUT) and wild-type littermate (WT) animals treated with or without DNA expression vector encoding CXCL12 $\gamma$  . Results are shown in ischemic (Isc) and non-ischemic (N.Isc) legs. Values are mean  $\pm$  SEM. n = 10 per group. A) 3 possible comparisons for Bonferroni correction, a value of  $p < 0.016$  was considered significant \* $p < 0.016$  versus WT. B-D) 15 possible comparisons for Bonferroni correction, a value of  $p < 0.003$  was considered significant. \*\* $p < 0.0006$  versus Isc WT, # $p < 0.003$ , ## $p < 0.0006$  versus Isc MUT.

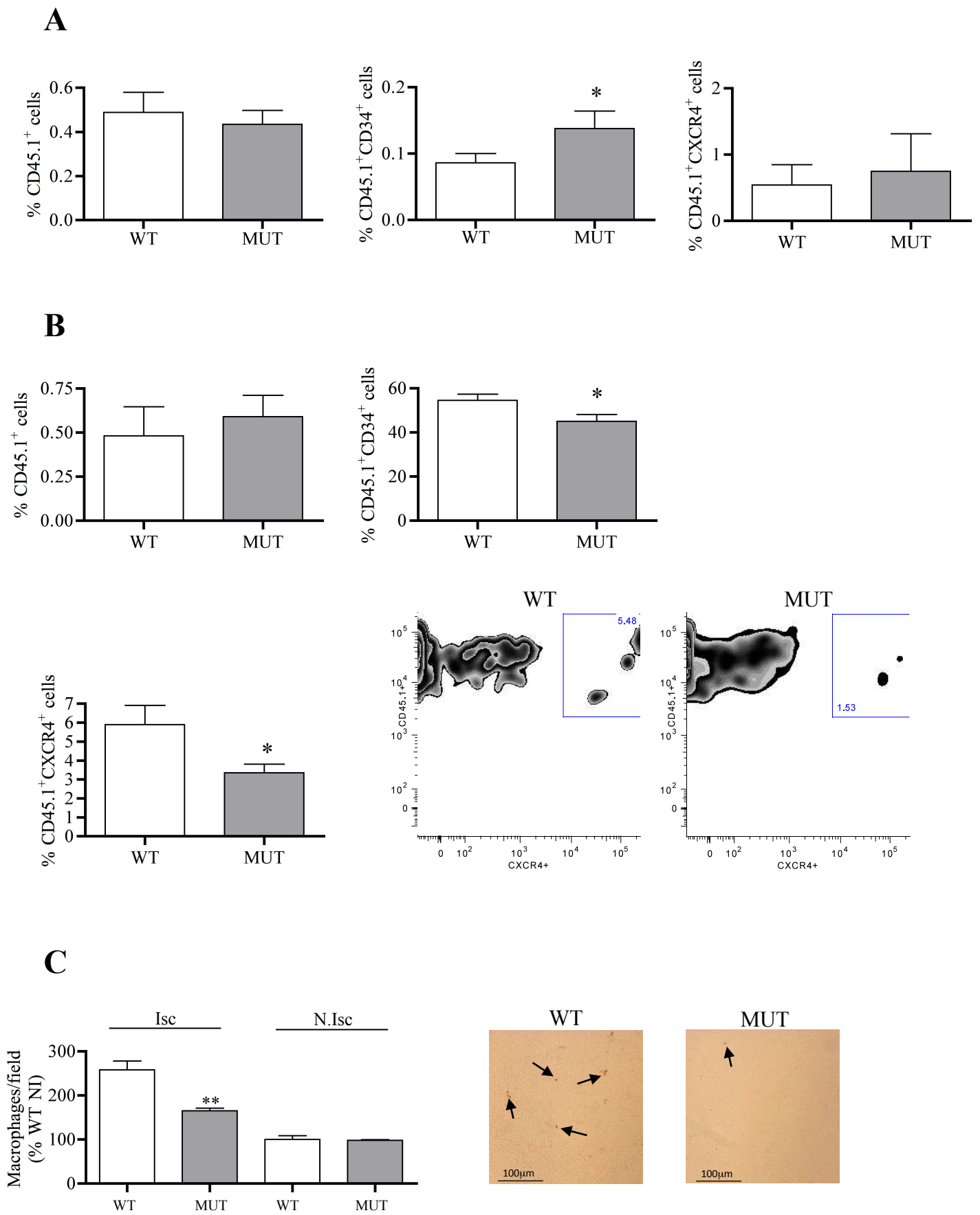


**Figure 1**

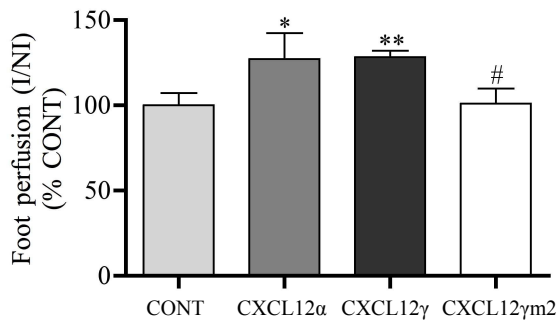
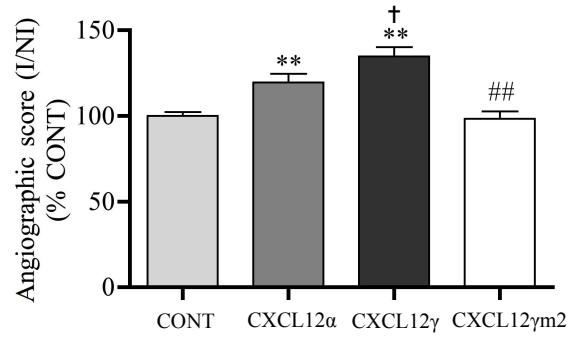
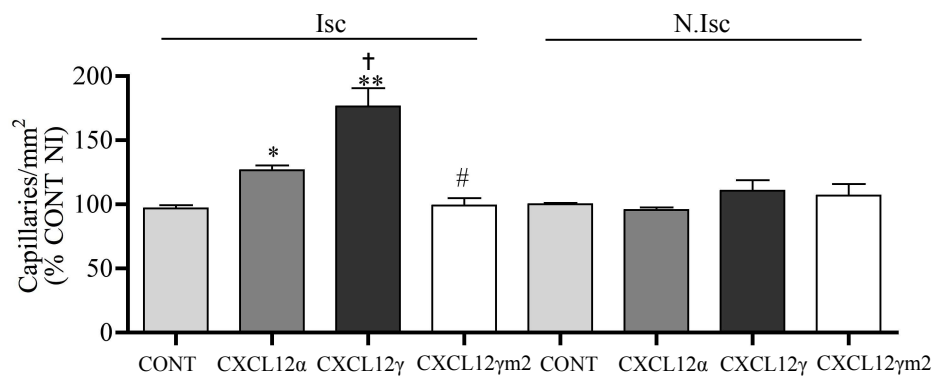
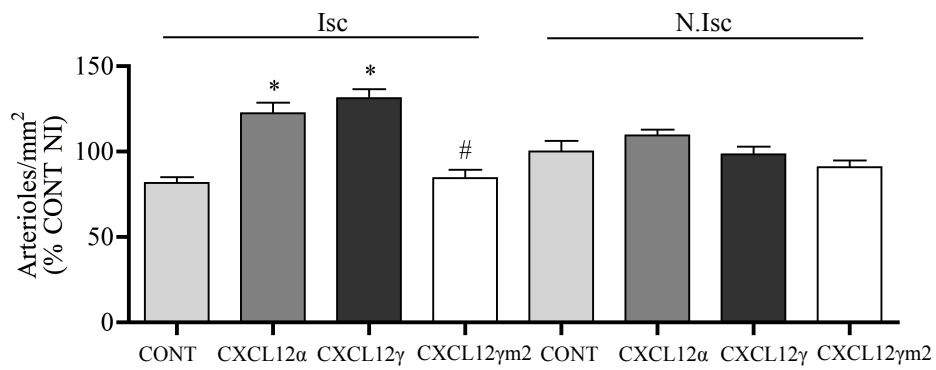
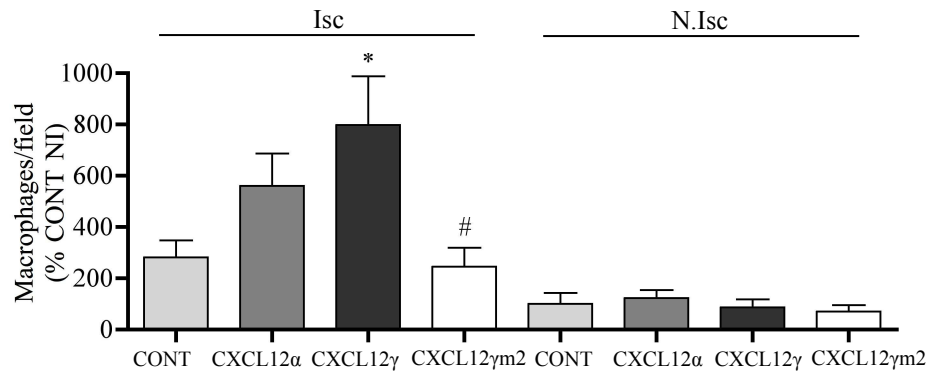




**Figure 3**



**Figure 4**

**A****B****C****D****E****Figure 5**

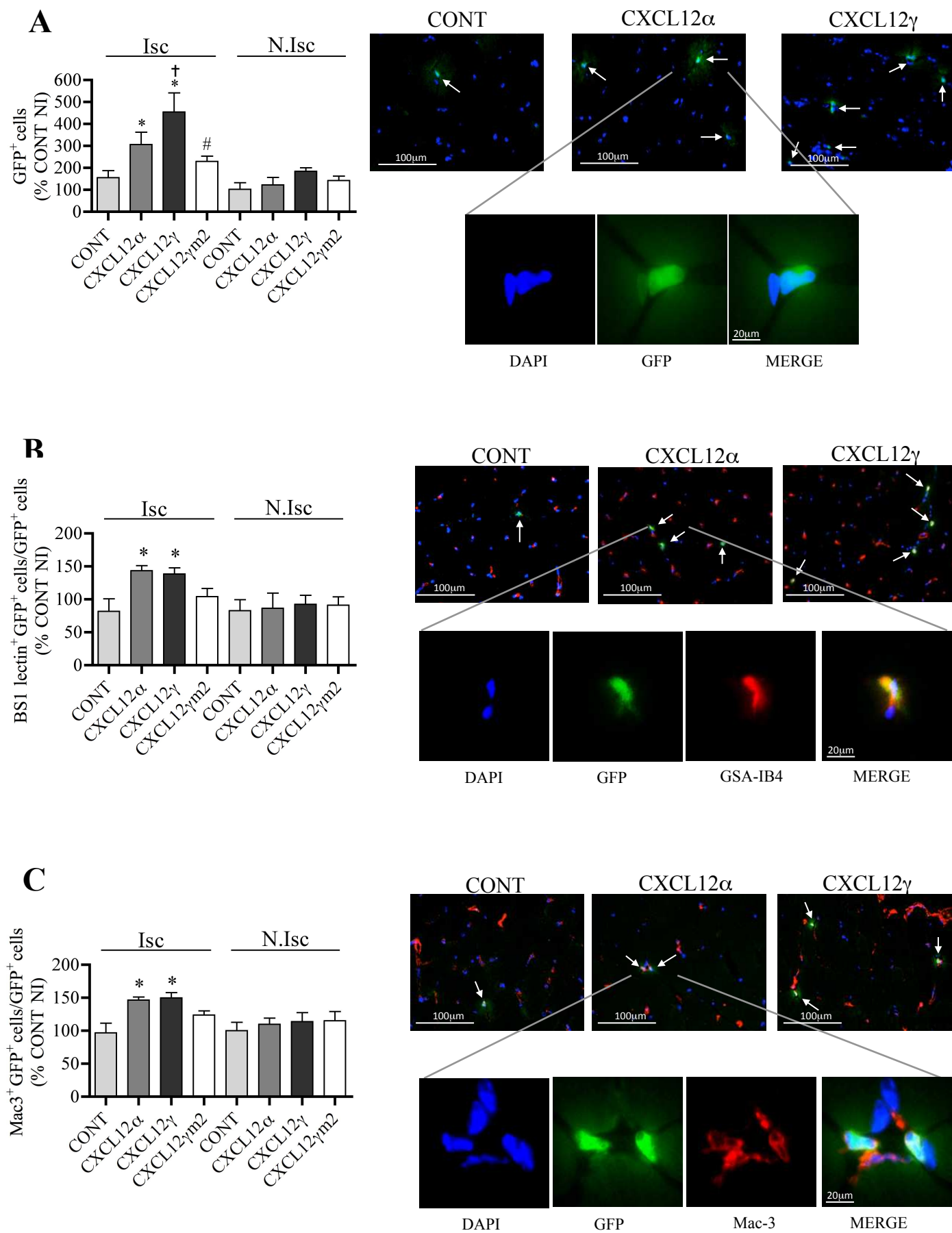


**Figure 6**

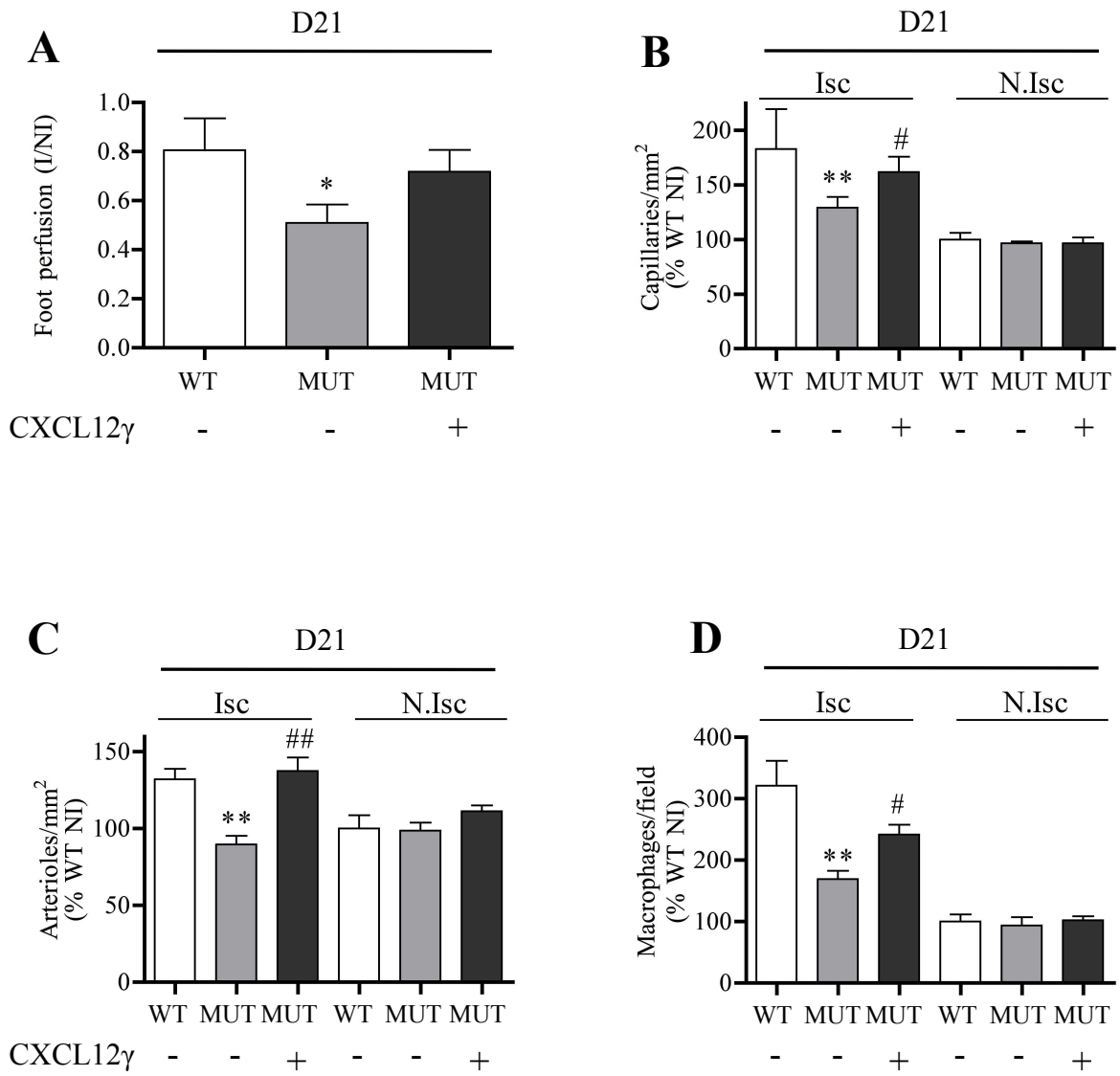
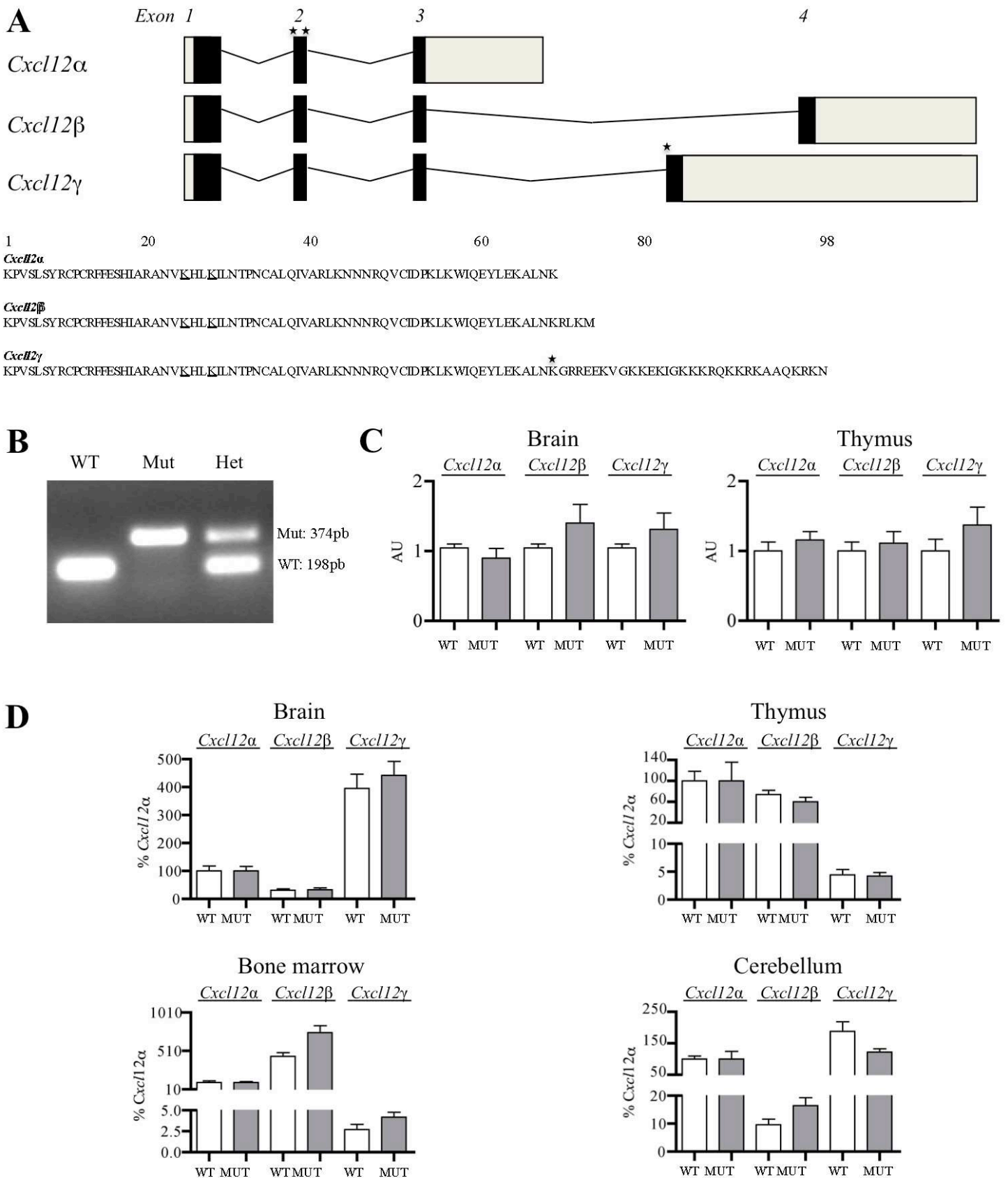


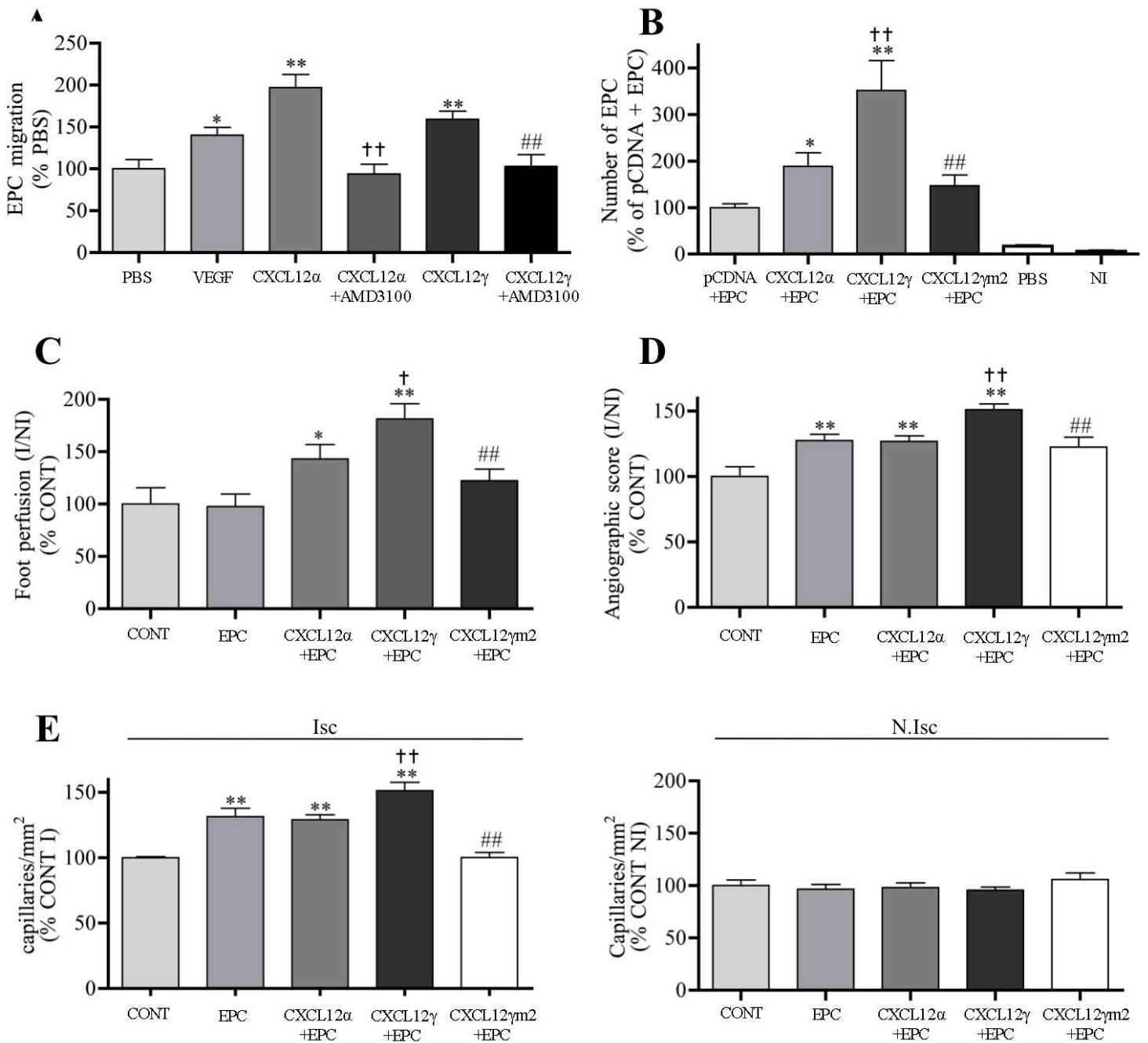
Figure 7

# Supplemental Material

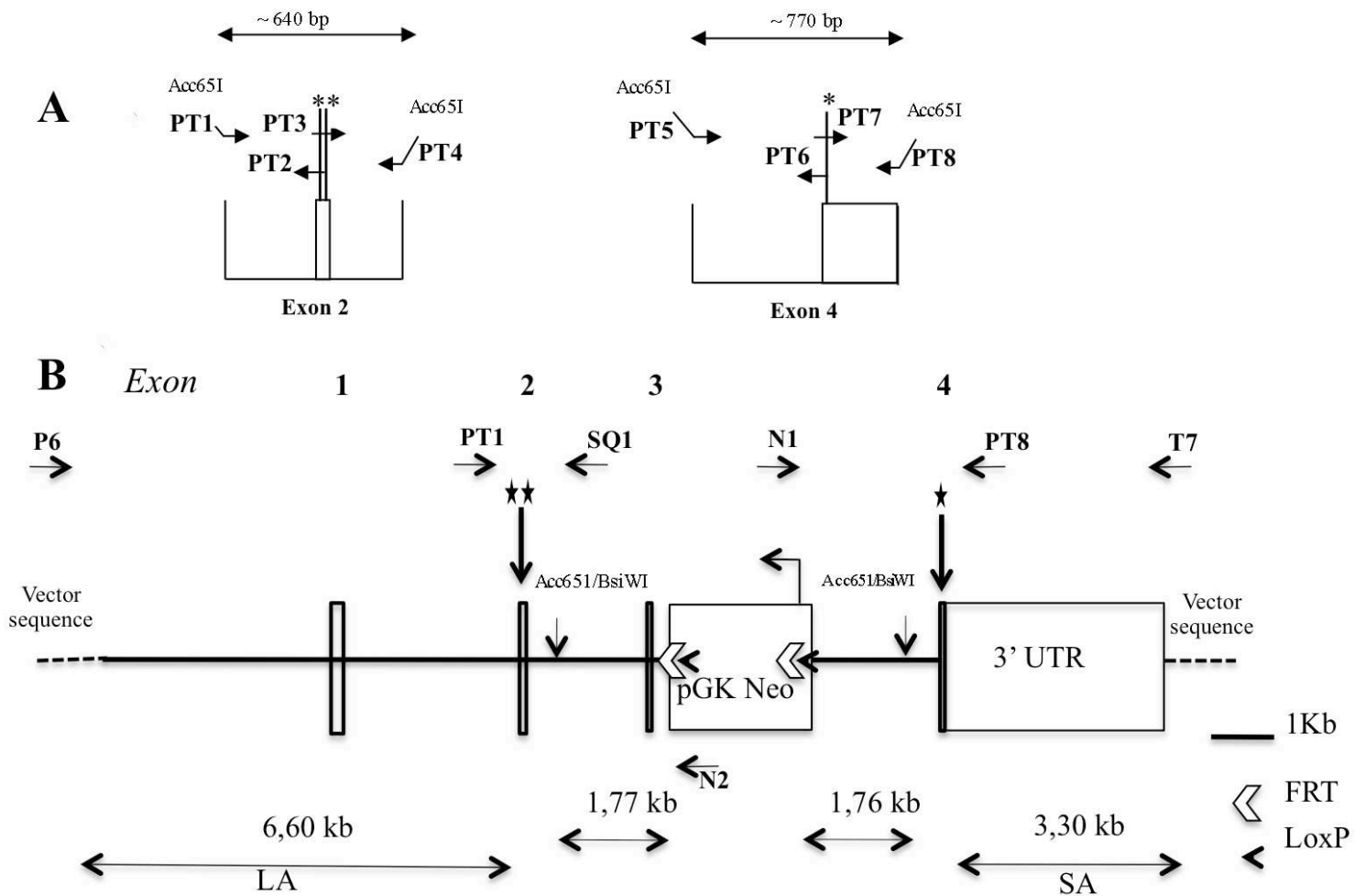


**Supplementary Figure 1. Characterization of *Cxcl12<sup>Gagtm/Gagtm</sup>* animals.** (A) Schematic diagram of *Cxcl12* isoforms structures and sequence alignment of the corresponding mature proteins. Mutations introduced in *Cxcl12<sup>Gagtm</sup>* are indicated (stars). In the amino-acid sequence the substituted residues corresponding to mutations are underlined. The incorporation of the non-sense mutation in the open reading frame of *Cxcl12<sup>γ</sup>* generates a truncated protein of 68Aa-length identical to *Cxcl12<sup>α</sup>*, which last aminoacid (K68) is marked by a star. (B) PCR amplification on genomic DNA from wild type (WT), *Cxcl12<sup>Gagtm/wt</sup>* (Het) and *Cxcl12<sup>Gagtm/Gagtm</sup>* (Mut) animals. (C-D) Real-time PCR analysis of *Cxcl12* products. (C) RNA expression levels of each isoform normalized to HPRT in brain and thymus tissues from WT and *Cxcl12<sup>Gagtm/Gagtm</sup>* animals. (D) mRNA levels of each *Cxcl12* isoform were normalized to that of *Cxcl12<sup>α</sup>*.





**Supplementary Figure 3. CXCL12 $\gamma$  controls EPC infiltration in ischemic tissues.** (a) Quantitative evaluation of EPC migration through transwell membrane in response to VEGF, CXCL12 $\alpha$  or CXCL12 $\gamma$ , in presence or absence of the synthetic CXCR4 antagonist, AMD3100 (5 $\mu$ M). n = 6 to 8 per group, representative of 2 independent experiments. \*p<0.05, \*\*p<0.01, \*\*\*p<0.001 versus PBS, ††† p<0.001 versus CXCL12 $\alpha$ , ## p<0.01 versus CXCL12 $\gamma$ . (b) Number of CFSE-stained human EPC (EPC) in the ischemic leg of C57BL/6 mice treated with intramuscular administration of cDNA expression vector encoding CXCL12 $\alpha$ , CXCL12 $\gamma$  or CXCL12 $\gamma$ m2, 4 days after the onset of ischemia. Quantitative evaluation of foot perfusion (c), microangiography (d) and capillary density (e), 14 days after ischemia in C57BL/6 mice treated with intravenous administration of EPC only or along with intramuscular cDNA expression vector encoding CXCL12 $\alpha$ , CXCL12 $\gamma$  or CXCL12 $\gamma$ m2. Empty DNA plasmid (CONT). Values are mean  $\pm$  SEM. n = 10 per group, representative of 2 independent experiments. 10 possible comparisons for Bonferroni correction, a value of p<0.005 was considered significant. \*p<0.005, \*\*p<0.001, versus CONT, † p<0.005, †† p<0.001 versus CXCL12 $\alpha$ +EPC, ##p<0.001 versus CXCL12 $\gamma$  + EPC.



**Supplementary Figure 4. Construction and sequencing validation of point mutation targeting vector of *Cxcl12*.** (a) Point mutations in 2<sup>nd</sup> and 4<sup>th</sup> exons were generated by 3-step PCR mutagenesis using PT1-PT4 and PT5-PT8 primers. The PCR fragments carrying mutations were then used to replace the correspondent wild type sequence using conventional sub cloning methods. (b) The boundaries of the two homology arms (LA , SA) were confirmed by sequencing with P6 and T7 primers that read through both sides of the backbone vector. The floxed Neo cassette was confirmed by sequencing with N1 and N2 primers that read from the 5'- and 3'- ends of the Neo cassette, respectively, into the genomic sequences. The mutations were confirmed by sequencing with PT1, SQ1 and PT8 primers. The sequencing results also proved that no other mutations were introduced into exon 2 and exon 4 before the natural stop codon.

#### Primers used to generate the point mutations (mutations are in bold and underlined)

PT1 (**Acc65I**): 5'- **ACTTGGTACCAACTTTCTGTAACCATTCTGC** -3'

PT2: 5'- **AGACAGATGCGAGACGTTGGCTCTGGCGATGTGGCTC** -3'

PT3: 5'- ACATCGCCAGAGCCAACGTCT**TCGCATCTGTCTATCCTCAACACTCCAACTGTG** -3'

PT4 (**Acc65I**): 5'- ACTTGGTACCCTCTGAGCAAGTGAGTGCAAGTG -3'

PT5 (**Acc65I**): 5'- **ACTTGGTACCTCTCTAGAACAATCTCAGTTATCC** -3'

PT6: 5'- **CTACCTTAGATAAAATTAGTAGAACC** -3'

PT7: 5'- GTTCTACTAATTTTATCTAAGG**TAG**GGGGCGCAGAGAAGAAAAAGTGG -3'

PT8 (**Acc65I**): 5'- ACTT**GGTACCAGAGTTTACCGTCAGGTTTGAGC** -3'

#### Sequencing Primer Sequences

Primer N1 5'-TGCGAGGCCAGAGGCCACTTGTGTAGC- 3'

Primer N2 5'-TTCCTCGTGCTTTACGGTATCG- 3'

Primer P6 5'-GAGTGCACCATATGGACATATTGTC- 3'

Primer T7 5'-TAATGCAGGTAACTGGCTTATCG- 3'

Primer PT1 5'-ACTT**GGTACCAACTTTCTGTAACCATTCTGC**- 3'

Primer SQ1 5'-ACAGGACACATCTCTGCCAAGTC- 3'

Primer PT8 5'-ACTT**GGTACCAGAGTTTACCGTCAGGTTTGAGC**- 3'